

MEASUREMENTS OF THE SPONTANEOUS
POLARIZATION IN KH_2PO_2

by

John Wesley Benepe

United States Naval Postgraduate School



THE SIS

MEASUREMENTS OF THE SPONTANEOUS
POLARIZATION IN KH_2PO_2

by

John Wesley Benepe

December 1970

This document has been approved for public release and sale; its distribution is unlimited.

T136821

Measurements of the Spontaneous Polarization in KH_2PO_2

by

John Wesley Benepe
Lieutenant Commander, United States Navy
B.A., Dartmouth College, 1961

Submitted in partial fulfillment of the
requirements for the degree of

DOCTOR OF PHILOSOPHY

from the
NAVAL POSTGRADUATE SCHOOL
December 1970

Thesis B 367
C.1

ABSTRACT

Measurements of the spontaneous polarization in KH_2PO_4 within 1K of the ferroelectric transition are reported. The measurements employed the electrocaloric effect, allowing simultaneous determination of the polarization and its temperature derivative. The derivative computed from polarization measurements compares well with direct determinations of $(\partial P/\partial T)_E$, demonstrating thermodynamic consistency of the measurements. The transition is first order with a discontinuous jump in the polarization of $1.87 \mu\text{C}/\text{cm}^2$ at the transition. Landau theory allows separate calculation of specific heat contributions of the lattice and polarization and thus the total specific heat, which agrees very well with direct calorimetric determinations, although the decomposition differs from that previously assumed. This indicates that Landau theory provides a good description of the transition in KH_2PO_4 and that there is a calorimetric anomaly not directly associated with the polarization. The free energy expansion best fitting the data contains P^4 and P^8 terms and no P^6 term.

TABLE OF CONTENTS

I.	INTRODUCTION-----	11
II.	THEORY-----	15
III.	METHODS FOR MEASURING THE SPONTANEOUS POLARIZATION--	29
	A. HYSTERESIS LOOPS-----	29
	B. INDIRECT MEASUREMENTS OF P_s in KDP-----	38
	1. Spontaneous Strain Measurements-----	38
	2. Electro-optic Measurements-----	40
	C. PYROELECTRIC TECHNIQUES-----	42
	D. ELECTROCALORIC TECHNIQUES-----	45
IV.	EXPERIMENTAL EQUIPMENT AND PROCEDURES-----	51
	A. CRYOSTAT AND THERMOMETRY-----	51
	B. APPARATUS FOR ELECTRICAL MEASUREMENTS-----	58
	C. SAMPLE PREPARATION-----	59
	D. EQUIPMENT OPERATION AND DATA ACCRUAL-----	61
	E. DATA REDUCTION AND ERROR ANALYSIS-----	64
V.	RESULTS AND CONCLUSIONS-----	72
APPENDIX I. THE EFFECT OF STRESS DUE TO ELECTRODES ON		
	THE FERROELECTRIC TRANSITION-----	85
APPENDIX II. EXPERIMENTAL DATA-----		87
LIST OF REFERENCES-----		88
INITIAL DISTRIBUTION LIST-----		90
FORM DD 1473 -----		91

LIST OF TABLES

I.	Relations Between Coefficients in the Linear Piezoelectric Equations-----	19
II.	Definitions of Coefficients in the Linear Piezoelectric Equations-----	19
III.	Values for the Parameters in the Landau Expansion--	77

LIST OF DRAWINGS

1.	The Polarization Dependence of the Free Energy-----	22
2.	The Field Dependence of the Polarization-----	24
3.	Some Spontaneous Polarization Measurements in KH_2PO_4 -----	30
4.	Sawyer-Tower Circuit for Measuring the Spontaneous Polarization-----	32
5.	A Typical Ferroelectric Hysteresis Loop-----	33
6.	Dielectric Hysteresis Loop Measurements in KH_2PO_4 -----	37
7.	Spontaneous Polarization as Calculated from the Spontaneous Strain in KH_2PO_4 -----	41
8.	Schematic Diagram of the Electrocaloric Apparatus for Making Polarization Measurements-----	47
9.	Measurements of P_s in Rochelle Salt-----	49
10.	Measurements of P_s^2 in Triglycine Sulfate-----	50
11.	Detailed Schematic Diagram of the Adiabatic Sample Chamber-----	52
12.	Schematic Diagram of the Adiabatic Thermostat-----	53
13.	Schematic Diagram of Temperature Measurement Apparatus-----	55
14.	Schematic of Electrocaloric Measurement Circuit-----	57
15.	Typical Sample Configuration-----	60
16.	Procedure for Normalizing Electrocaloric Polarization Data-----	65
17.	P^2 vs ΔT Data-----	66
18.	P_s^2 vs $(T_c - T)$ -----	68
19.	Some $(\partial T / \partial E)_S$ vs E Data-----	70
20.	$(\partial T / \partial E)_S$ vs $(T_c - T)$ -----	71

21.	The Spontaneous Polarization in KH_2PO_4 -----	73
22.	$\text{Log } P_s$ vs $\text{Log } (T_c - T)$ -----	74
23.	The Spontaneous Polarization Compared With a Two Parameter Fit to Landau Theory-----	76
24.	The "Saturation Function" in KH_2PO_4 -----	79
25.	$(\partial P / \partial T)_E$ vs $(T_c - T)$ -----	80
26.	The Specific Heat in KH_2PO_4 -----	82

ACKNOWLEDGEMENTS

This thesis is the culmination of four years at the Naval Postgraduate School. For me, these years have held some trying and some rewarding moments. The faculty and staff of the Physics Department have done much to make the rewarding moments the more frequent. In particular I wish to thank Professor Gordon Schacher, Mr. Lyn May, and my thesis advisor, Professor William Reese for seeing me through the trying times and enjoying the better times with me. To Lyn go my additional thanks for help in things technical and I hopefully will leave here more dexterous in the use of my many thumbs. Most of physical insight which I possess is due to the tutelage of Professor Reese and without his advice and prodding I could never have finished this thesis.

I. INTRODUCTION

There has been much recent interest in the study of phase transitions. In the temperature region near a phase transition, many of the physical properties of a system undergo very rapid changes. Measurements of the properties in this region provide a sensitive measure of the competing interactions responsible for the transition and lead to a better understanding of the behavior of the system at all temperatures.

The free energy of a system must be continuous at a phase transition; however, its derivatives may exhibit discontinuities. A transition which is described by a free energy having a discontinuity in one of its first derivatives is known as first order, while one where the first derivatives are all continuous and there is a discontinuity in one of the second derivatives is known as second order.

Ferroelectrics are a class of crystals which undergo a phase transition from the ordinary paraelectric phase to a so-called ferroelectric phase at some well defined transition temperature, T_c . The paraelectric phase is usually the high temperature one. In the ferroelectric phase, the crystal is characterized by the possession of a reversible permanent electrical dipole moment or spontaneous polarization, P_s . The polarization can be reversed by the application of an external electric field and the relation between P and E obtained in the process exhibits hysteresis very similar to that between B and H in a ferromagnet. This is the only analogy between a ferromagnet and ferroelectric.

This dissertation reports on the results of an effort to make unambiguous measurements of the spontaneous polarization in Potassium Dihydrogen Phosphate (KH_2PO_4 or more commonly KDP) in the temperature region very close to its transition temperature.

It is commonly believed that the mechanism for the ferroelectric phase transition is the existence of an instability in the crystal lattice which leads to a lowering of the lattice symmetry, with an accompanying lattice distortion, at T_c . This distortion is called the spontaneous strain and it is directly related to the spontaneous polarization.

The lattice instability is generally ascribed to one of two causes. In so-called displacive ferroelectrics, it is thought that the long range electrostatic forces in the crystal, generated by the polarization induced by a transverse optical phonon mode, tend to reinforce the lattice deformation due to the phonon. The result is a permanent lattice deformation at the transition temperature. Cochran [1] has developed this theory in detail and it seems to describe the transition in Barium Titanate (BaTiO_3) very well. In so-called order-disorder ferroelectrics, the instability is due to a tendency for dipoles to order as the temperature decreases. In ferroelectrics with hydrogen bonds, the protons may have a tendency to order in a double minimum potential well in the bond, leading to an ordered state below T_c . The transition in Triglycine Sulfate (TGS) seems to be due to this mechanism.

In KDP, both these mechanisms play a role. X-ray [2] and neutron [3] diffraction data indicate that, while the ordering of the protons in the hydrogen bonds is a significant factor in the transition, the spontaneous polarization is entirely due to ionic displacements. The statistical theory of ferroelectricity in KDP as developed by Slater [4], and refined by Takagi [5] and Silsby et.al. [6], is basically of the Ising model from and assumes that there is a one-to-one correspondence between the polarization and the degree of proton ordering in the hydrogen bonds, even though the polarization is along the crystal c-axis and the ordering takes place in the a-b plane.

KDP is tetragonal above T_c , and orthorhombic below with the spontaneous strain being an x_y shear. (For more details on the crystal structure and physical properties see Refs. [7][8][9][10].) Associated with this change in lattice symmetry are anomalies in many of the physical properties. Above T_c , the dielectric susceptibility along the c-axis exhibits a Curie law temperature dependence, $\chi = C/(T-\theta)$, as do the piezoelectric strain coefficient and components of the tensor of elastic compliances associated with an x_y strain. Below T_c , the values of these properties decrease again, but in a more complicated fashion. The specific heat rises sharply below T_c and drops very sharply at the transition. These anomalies in the physical properties are related to one another via thermodynamics by the phenomenological theory of ferroelectricity, which assumes a particular form for the thermodynamic free energies.

The most reliable previous measurements of the spontaneous polarization (discussed in Chapter II) were made in 1943 with rather poor temperature resolution. They do not agree well thermodynamically with the recent, more accurate, specific heat measurements of Strukov [11] and Reese [12]. In addition, they indicate that P_s drops sharply but continuously to zero at T_c indicating that the transition is second order. Recent dielectric measurements [13][14] and Reese's measurement of a latent heat at the transition indicate that the transition is first order. Accurate polarization measurements with good temperature resolution in the temperature region very close to T_c were needed to resolve these differences.

A thorough survey of previous measurements and techniques was made and it was decided that the electrocaloric effect could best be employed to measure P_s . The method used allowed a thermodynamic check on the internal consistency of the measurements and on the validity of the phenomenological theory of ferroelectrics as applied to KDP. The measurements confirm that the transition is first order and indicate that previous measurements are in serious error in the region less than 1.0K from T_c . The phenomenological theory is found to hold to within 10^{-3} K of T_c .

The next chapter covers the phenomenological theory of KDP as a prelude to a discussion and comparison of previous measurements in Chapter III. Chapter IV contains a description of the equipment and technique used in this experiment and Chapter V presents the results and some conclusions derived from them.

II. THEORY

The phenomenological theory of ferroelectricity was first developed by Mueller [15] and Cady [16], for Rochelle salt. They assumed equations of state which are expansions of free energy functions in terms of the appropriate thermodynamic variables. These free energy functions are not related by Legendre transformations, however, and so the thermodynamic variables appearing in the resulting equations are not the macroscopically observable ones. Devonshire has developed a thermodynamically consistent formulation [17], but has applied it only to the case of BaTiO_3 which has a multiaxial polarization and is not piezoelectric above its transition. In the special case of a stress free crystal both of these formulations reduce to a special case of Landau's general theory of phase transitions [18], where the polarization plays the role of the order parameter. Since a correct formulation of the phenomenological theory for KDP does not exist in the literature, it will be developed from first principles here.

The first law of thermodynamics gives, for a stressed dielectric in an external field:

$$dU = TdS + \vec{E} \cdot d\vec{P} + \sum_{ij} X_i dx_{ij} ,$$

where U is the internal energy density, \vec{E} and \vec{X} are the externally applied field and stress, \vec{P} is the polarization and x_{ij} is a strain component in the dielectric, and S is the entropy density.

For KDP, the only components relating to the ferroelectric behavior are E_z , P_z , X_y , and x_y . Since these are the only components in which we are interested, we disregard the rest and drop the subscripts, obtaining:

$$dU = TdS + EdP + Xdx. \quad (1)$$

E and X are the externally applied field and stress; P and x are the total polarization and strain. S is the entropy density. Using Legendre transformations on Equation (1) we obtain:

$$dA = -SdT + EdP + Xdx, \quad (2)$$

$$dG_1 = -SdT + EdP - xdx, \quad (3)$$

$$dG_2 = -SdT - PdE + Xdx, \quad (4)$$

$$dG = -SdT - PdE - xdx, \quad (5)$$

where:

$A = U - TS$ = Helmholtz free energy density,

$G_1 = A - Xx$ = elastic Gibbs free energy density,

$G_2 = A - EP$ = electric Gibbs free energy density,

$G = G_1 - EP$ = total Gibbs free energy density.

We can obtain the following relations from Equation (2) - (5):

$$E = (\partial A / \partial P)_{T,S} = (\partial G_1 / \partial P)_{T,X}, \quad (6)$$

$$P = -(\partial G_2 / \partial E)_{T,x} = -(\partial G / \partial E)_{T,X}, \quad (7)$$

$$X = (\partial A / \partial x)_{T,P} = (\partial G_2 / \partial x)_{T,E}, \quad (8)$$

$$x = -(\partial G_1 / \partial X)_{T,P} = -(\partial G / \partial X)_{T,E}, \quad (9)$$

$$S = -(\partial F / \partial T) \text{ all other var. const.}, \quad (10)$$

where F is any of the free energy functions.

For equations of state we expand the free energy functions in terms of their natural variables, leaving the temperature dependence in the expansion coefficients. As a first approximation we expand bilinearly, getting:

$$A = \frac{1}{2} C^P x^2 + \frac{1}{2} k^X P^2 - aPx, \quad (11)$$

$$G_1 = -\frac{1}{2} S^P X^2 + \frac{1}{2} k^X P^2 - bPX, \quad (12)$$

$$G_2 = \frac{1}{2} C^E x^2 - \frac{1}{2} \chi^X E^2 - eEx, \quad (13)$$

$$G = -\frac{1}{2} S^E X^2 - \frac{1}{2} \chi^X E^2 - dEX. \quad (14)$$

Using Equations (6) - (9) and (11) - (14) gives:

$$x = S^P X + bP, \quad (15a) \qquad x = S^E X + dE, \quad (16a)$$

$$E = -bX + k^X P, \quad (15b) \qquad P = dX + \chi^X E, \quad (16b)$$

$$X = C^P x - aP, \quad (15c) \qquad X = C^E x - eE, \quad (16c)$$

$$E = -ax + k^X P, \quad (15d) \qquad P = ex + \chi^X E. \quad (16d)$$

The definitions of the coefficients are given in Table II and the relations between them which can be derived from the above equations are given in Table I.

Equations (15) and (16) are called the linear piezoelectric equations. They do not describe ferroelectric behavior because they cannot yield a spontaneous polarization. To describe ferroelectricity we must add higher order terms in the free energy expansions.

Experimentally we find that the coefficients S^E , C^E , χ^X , χ^X , k^X , k^X , e , and d all show anomalous temperature dependence near T_c in ferroelectrics, while a , b , C^P , S^P are nearly temperature

independent. This being the case, if we use A and G_1 for equations of state for ferroelectrics, we need only add higher order terms in P to get ferroelectric behavior, whereas if we use G_2 or G the situation is much more complicated.

Thus, we choose A and G_1 for our equations of state and add higher powers of P , giving:

$$A = \frac{1}{2} C^P x^2 - aPx + \frac{1}{2} k^X P^2 + \Phi(P), \quad (17)$$

$$G_1 = -\frac{1}{2} S^P X^2 - bPX + \frac{1}{2} k^X P^2 + \Phi(P). \quad (18)$$

$\Phi(P)$ contains only even orders of P since the polarization in a ferroelectric is reversible, thus a change in the sign of P cannot affect the free energy. We also assume $\Phi(P)$ to be independent of temperature. Thus:

$$\Phi(P) = \frac{\beta}{4} P^4 + \frac{\gamma}{6} P^6 + \frac{\delta}{8} P^8 + \dots \quad (19)$$

$\Phi(P)$ is the same in (17) and (18) because A and G_1 are related by a Legendre transformation not involving P .

Using Equations (2) - (5), we obtain:

$$x = S^P X + bP, \quad (20a)$$

$$E = -bX + k^X P + \Phi'(P), \quad (20b)$$

$$X = C^P x - aP, \quad (20c)$$

$$E = -ax + k^X P + \Phi'(P), \quad (20d)$$

where:

$$\Phi'(P) = \partial\Phi(P)/\partial P.$$

TABLE I

Relations between coefficients in the linear piezoelectric equations.

$$\begin{array}{ll}
 k^X = \frac{1}{\chi^X} & b = aS^P \\
 k^x = \frac{1}{\chi^x} & d = eS^E \\
 & d = b\chi^X \\
 & e = a\chi^x \\
 C^P = \frac{1}{S^P} & \chi^X - \chi^x = ed \\
 & k^x - k^X = ab \\
 C^E = \frac{1}{S^E} & S^E - S^P = bd \\
 & C^P - C^E = ae
 \end{array}$$

TABLE II

Definitions of coefficients in the linear piezoelectric equations.

Note: superscript indicates the variable held constant.

$$\begin{array}{ll}
 \chi = \chi_{33} = \text{dielectric susceptibility} \\
 k = k_{33} = \text{reciprocal dielectric susceptibility} \\
 C = C_{66} = \text{elastic constant} \\
 S = S_{66} = \text{elastic compliance} \\
 a = a_{36} = \text{piezoelectric stress constant} \\
 b = b_{36} = \text{piezoelectric strain constant} \\
 d = d_{36} = \text{piezoelectric strain coefficient} \\
 e = e_{36} = \text{piezoelectric stress coefficient}
 \end{array}$$

In Equation (20), x is the total strain (including the spontaneous strain x_s) referred to the unstressed state above T_c , P is the total polarization (including P_s), and E and X are the externally applied electric field and stress. The spontaneous polarization and strain are obtained by setting $E = 0$ and $X = 0$, yielding:

$$P_s = \Phi'(P_s)/k^{X=0}, \quad (21a)$$

$$x_s = bP_s. \quad (21b)$$

In Equations (20), k^X and k^x are no longer the total reciprocal susceptibilities because of the higher order terms in $\Phi'(P)$. Above T_c for small applied fields, $1/\chi \cong k$ since P is small and thus $\Phi'(P)$ is nearly zero.

Let us now treat the case of a free crystal. Experimentally, we know that above T_c the isothermal susceptibility follows a Curie law for small fields, i.e.:

$$\chi_T = \frac{C}{T-\theta},$$

where C is the Curie constant, and θ is the Curie temperature. This suggests that $k^{X=0} = \alpha(T-\theta)$, where α is some constant independent of temperature. We then write for G_1 or \dot{A} (the two are equivalent for $X = 0$):

$$\begin{aligned} G_1' &= G_0 + \frac{1}{2} \alpha(T-\theta)P^2 + \Phi(P) \\ &= G_0 + \frac{1}{2} \alpha(T-\theta)P^2 + \frac{\beta}{4}P^4 + \frac{\gamma}{6}P^6 + \dots \end{aligned} \quad (22)$$

where G_1' is the free energy density for $X = 0$ and we have included G_0 , the free energy of the lattice. The electric field is:

$$E = \alpha(T-\theta)P + \Phi'(P) = \alpha(T-\theta)P + \beta P^3 + \gamma P^5 + \dots \quad (23)$$

The isothermal reciprocal susceptibility is:

$$\frac{1}{\chi_T} = \alpha(T-\theta) + \Phi''(P) = \alpha(T-\theta) + 3\beta P^2 + 5\gamma P^4 + \dots \quad (24)$$

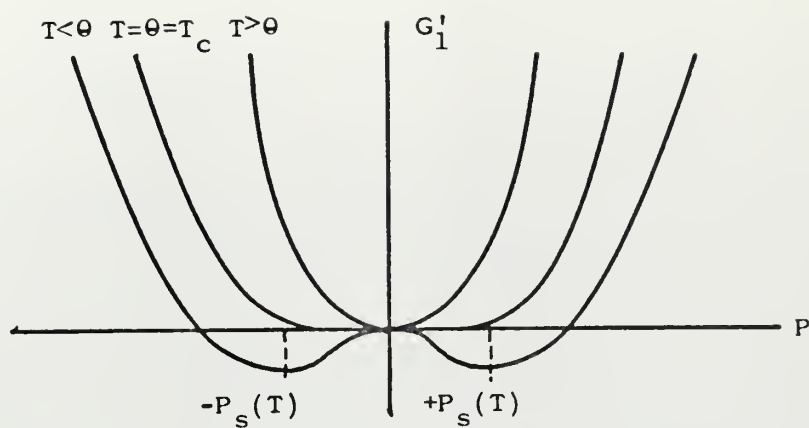
To simplify the treatment let us neglect the terms of G'_1 higher than P^6 . We take all the coefficients in Equation (22) to be positive with the exception of β . The sign of β determines the order of the transition. From Figure 1a, we see that for $\beta > 0$, the minimum of G'_1 corresponds to $P_s \neq 0$ for $T < \theta$. For $T > \theta$ the minimum is zero. Thus P_s goes continuously from zero at θ to non-zero values for $T < \theta$. The transition is second order and $\theta = T_c$. For $\beta < 0$ (see Figure 1b), at $T = T_c$ the polarization can be zero or $\pm P_s(T_c)$. Thus P_s rises discontinuously and the transition is first order. Notice also that for $\beta < 0$, θ is less than T_c . The treatment that follows is for the first order transition. The second order case is simpler and will not be discussed.

We solve for the spontaneous polarization by setting $E = 0$ in Equation (23), obtaining:

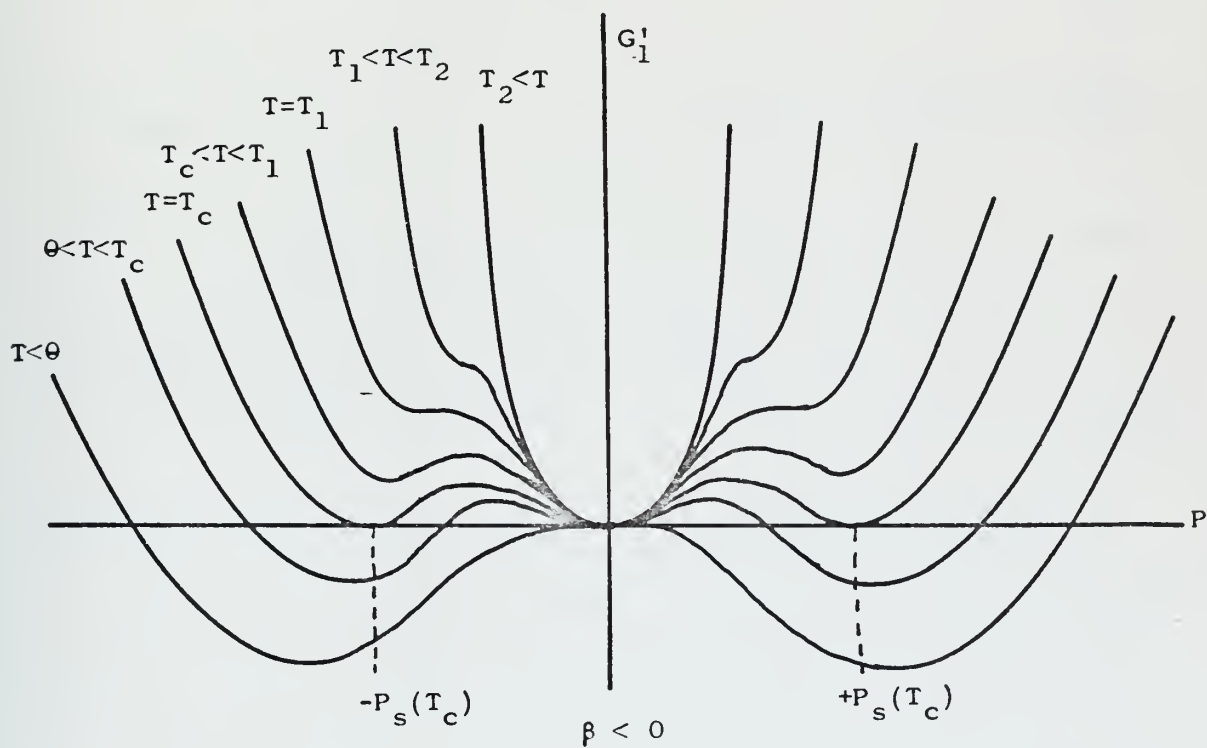
$$P_s^2(T) = -\frac{\beta}{2\gamma} \left[1 + \left\{ 1 + 4 \frac{\alpha\gamma}{\beta^2} (\theta - T) \right\}^{\frac{1}{2}} \right]. \quad (25)$$

If we put this result into Equation (24) we get the reciprocal susceptibility for small fields below T_c :

$$\frac{1}{\chi_T} = -4\alpha(T-\theta) + \frac{\beta^2}{\gamma} \left[1 + \left\{ 1 + 4 \frac{\alpha\gamma}{\beta^2} (\theta - T) \right\}^{\frac{1}{2}} \right]. \quad (26)$$



(a): $\beta > 0$
2nd Order



(b): 1st Order

Figure 1. The Polarization Dependence of the Free Energy

At $T = \theta$ we have from Equations (25) and (26):

$$P_S^2(\theta) = -\beta/\gamma, \quad (27a)$$

$$1/\chi_\theta = 2\beta^2/\gamma. \quad (27b)$$

At $T = T_c$ we must solve two equations:

$$\frac{1}{2} \alpha(T_c - \theta) P_S^2(T_c) + \frac{1}{4} \beta P_S^4(T_c) + \frac{1}{6} \gamma P_S^6(T_c) = 0,$$

$$\alpha(T_c - \theta) P_S(T_c) + \beta P_S^3(T_c) + \gamma P_S^5(T_c) = 0,$$

whose solutions are:

$$P_S^2(T_c) = -\frac{3}{4} \beta/\gamma, \quad (28a)$$

$$T_c - \theta = \frac{3}{16} \beta^2/\alpha\gamma. \quad (28b)$$

Above T_c , $1/\chi_T = \alpha(T - \theta)$. Putting Equation (28b) into this we get:

$$1/\chi_{T_c} = \frac{3}{16} \beta^2/\gamma. \quad (29a)$$

From Equations (26) and (28b) we have:

$$1/\chi_{T_c}^- = \frac{3}{4} \beta^2/\gamma. \quad (29b)$$

Equations (29) show that $1/\chi_T$ has a discontinuous rise at T_c .

The relation between E and P is very non-linear in the region near T_c . Figure 2 shows the relation for various temperatures. According to Maxwell's rule of equal areas, when the polarization reaches point A it jumps to point B as E goes in the negative direction. Between T_c and T_1 there exists a metastable polar state.

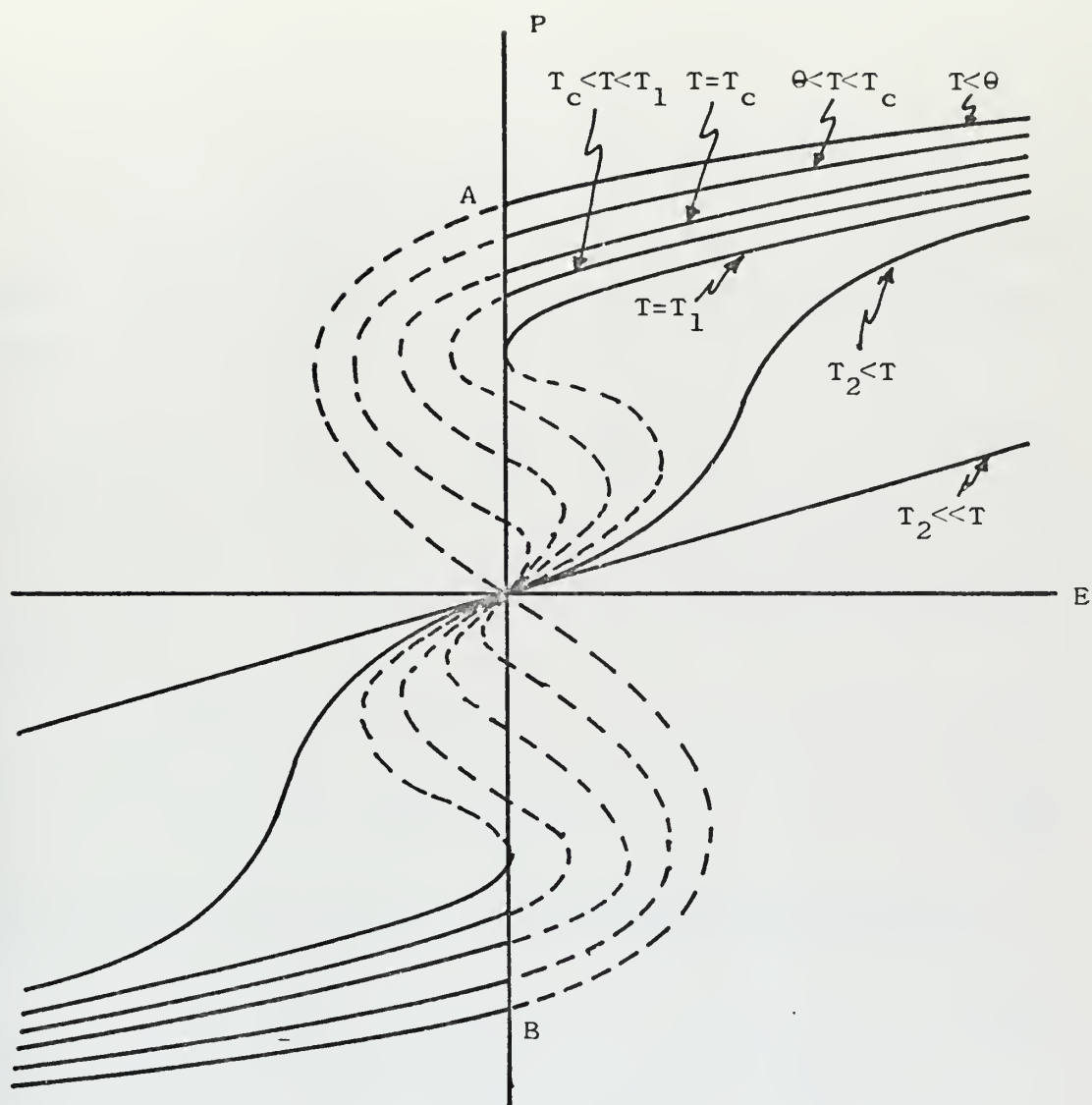


Figure 2. The Field Dependence of the Polarization

At T_1 this becomes a point of inflection which disappears at T_2 . As can be seen, it is very difficult to determine from E vs P data whether there is a spontaneous polarization for $E = 0$ or not. (This problem is more fully discussed in Chapter III.)

In the preceding discussion we have omitted all terms in G'_1 higher than P^6 . In Chapter V we shall need to make use of the solutions for P_s from the equation:

$$G'_1 = G_0 + \frac{\alpha}{2} (T-\theta)P^2 + \frac{\beta}{4}P^4 + \frac{\delta}{8}P^8, \quad (30)$$

where γ , the coefficient of P^6 , is zero and we use the next term in the expansion. We get, using Equation (30), the following results:

$$P_s^4(T_c) = -\frac{2}{3} \beta/\delta, \quad (31a)$$

$$T_c - \theta = -\frac{1}{3} \frac{\beta}{\alpha} P_s^2(T_c). \quad (31b)$$

From Equation (30) we obtain the following equation for P_s :

$$P_s^6 + \frac{\beta}{\delta} P_s^2 + \frac{\alpha}{\delta} (T-\theta) = 0. \quad (32)$$

Using (31) in (32) we obtain:

$$P_s^6 - \left(\frac{3}{2} P_s^4(T_c)\right)P_s^2 + \left(\frac{1}{2} \frac{P_s^6(T_c)}{T_c - \theta}\right)(T-\theta) = 0. \quad (33)$$

Thus if we know $(T_c - \theta)$ and $P_s(T_c)$ we can solve Equation (33) for P_s at any value of $(T-\theta)$.

Using Equations (10) and (22), we obtain for the entropy:

$$S = S_0 - \frac{1}{2} \alpha P^2, \quad (34)$$

where S_0 is the entropy not due to the polarization.

The specific heat at constant field is:

$$C_E = C_P - \frac{1}{2} \alpha T (\partial(P^2)/\partial T)_E, \quad (35)$$

where $C_P = T(\partial S_O/\partial T)$ is the specific heat at constant polarization.

The latent heat at the transition is:

$$L = T_C \Delta S(T_C) = \frac{1}{2} \alpha (T_C P_S^2(T_C)). \quad (36)$$

Ferroelectrics display a large electrocaloric effect near T_C . This effect can be used to measure the spontaneous polarization. According to thermodynamics:

$$dS = (\partial S/\partial T)_E dT + (\partial S/\partial E)_T dE, \quad (37a)$$

$$dS = (\partial S/\partial T)_P dT + (\partial S/\partial P)_T dP. \quad (37b)$$

For an adiabatic process, $dS = 0$. Using the Maxwell relations:

$$(\partial S/\partial P)_T = - (\partial E/\partial T)_P,$$

$$(\partial S/\partial E)_T = (\partial P/\partial T)_E.$$

We find from Equations (37) that:

$$dT = - (T/C_E) (\partial P/\partial T)_E dE, \quad (38a)$$

$$dT = (T/C_P) (\partial E/\partial T)_P dP. \quad (38b)$$

These are the equations governing the electrocaloric effect. They show that, under adiabatic conditions, if we decrease the entropy due to the polarization by applying a field, the entropy of the lattice, and thus its temperature, must increase in order to keep the entropy of the crystal constant.

From Equation (23), we have that:

$$(\partial E / \partial T)_P = \alpha P,$$

so that Equation (38b) becomes:

$$dT = (\alpha T / 2C_P) d(P^2). \quad (39)$$

Thus, we find that the electrocaloric temperature change is proportional to the square of the polarization. This result is quite general and depends only on the fact that the free energy must be invariant under a polarization reversal and on the way we chose to include the temperature dependence. In the most general case we would have $\Delta T = f(P^2)$ where f may include some non-linear terms.

From Equation (35) we find:

$$C_E = C_P - \alpha T P (\partial P / \partial T)_E. \quad (40)$$

From Equation (38a) we obtain:

$$(\partial T / \partial E)_S = - (T / C_E) (\partial P / \partial T)_E, \quad (41)$$

and from Equation (39):

$$C_P = \alpha T / 2 (\partial T / \partial (P^2))_S. \quad (42)$$

Thus, electrocaloric measurements allow a calculation of the total specific heat of the crystal since P , $(\partial P / \partial T)_E$, and $(\partial T / \partial (P^2))_S$ can all be obtained from experimental data.

From Equations (40) and (41) we obtain:

$$P = \frac{C_E - C_P}{C_E} [\alpha (\partial T / \partial E)_S]^{-1}. \quad (43)$$

Thus, measurements of $(\partial T / \partial E)_S$ allow a calculation of the polarization. This value can be compared with the polarization measured using $(\partial T / \partial (P^2))_S$ data (explained in Chapter IV), allowing a check on the thermodynamic consistency of electrocaloric measurements and a check on the validity of Landau theory.

The entirety of the above phenomenological theory assumes a single domain crystal. There is as yet no successful theory which includes domain effects in its treatment. The complications which arise in real crystals due to domains are discussed in the next chapter.

III. METHODS FOR MEASURING THE SPONTANEOUS POLARIZATION

All previous direct and indirect measurements of the spontaneous polarization in KDP have been made isothermally, employing thermostats with temperature control reported to be 0.01K at best. Within 1K of T_c such measurements are not sufficiently accurate to determine the details of the temperature dependence of P_s , which changes very rapidly in this temperature region. The difference between the various measurements becomes exaggerated in this region, as indicated in Figure 3. This chapter contains a discussion of the various methods used to determine P_s in KDP and some different techniques which have been used to make measurements in other ferroelectrics.

A. HYSTERESIS LOOPS

The most common method for measuring P_s directly employs the ferroelectric property of hysteresis. The method was first developed by Sawyer and Tower [19] and has been used by von Arx and Bantle [20] and Gonzalo [21] in KDP.

With no electric field applied, a domain structure forms in a ferroelectric crystal. In KDP, the polarization in adjacent domains is reversed. (KDP has a uniaxial polarization. In BaTiO_3 which has a multiaxial polarization, the polarization in adjacent domains is differently oriented but not necessarily reversed.) As an electric field is applied to the sample, the domains whose polarization has the same polarity as the field grow at the expense

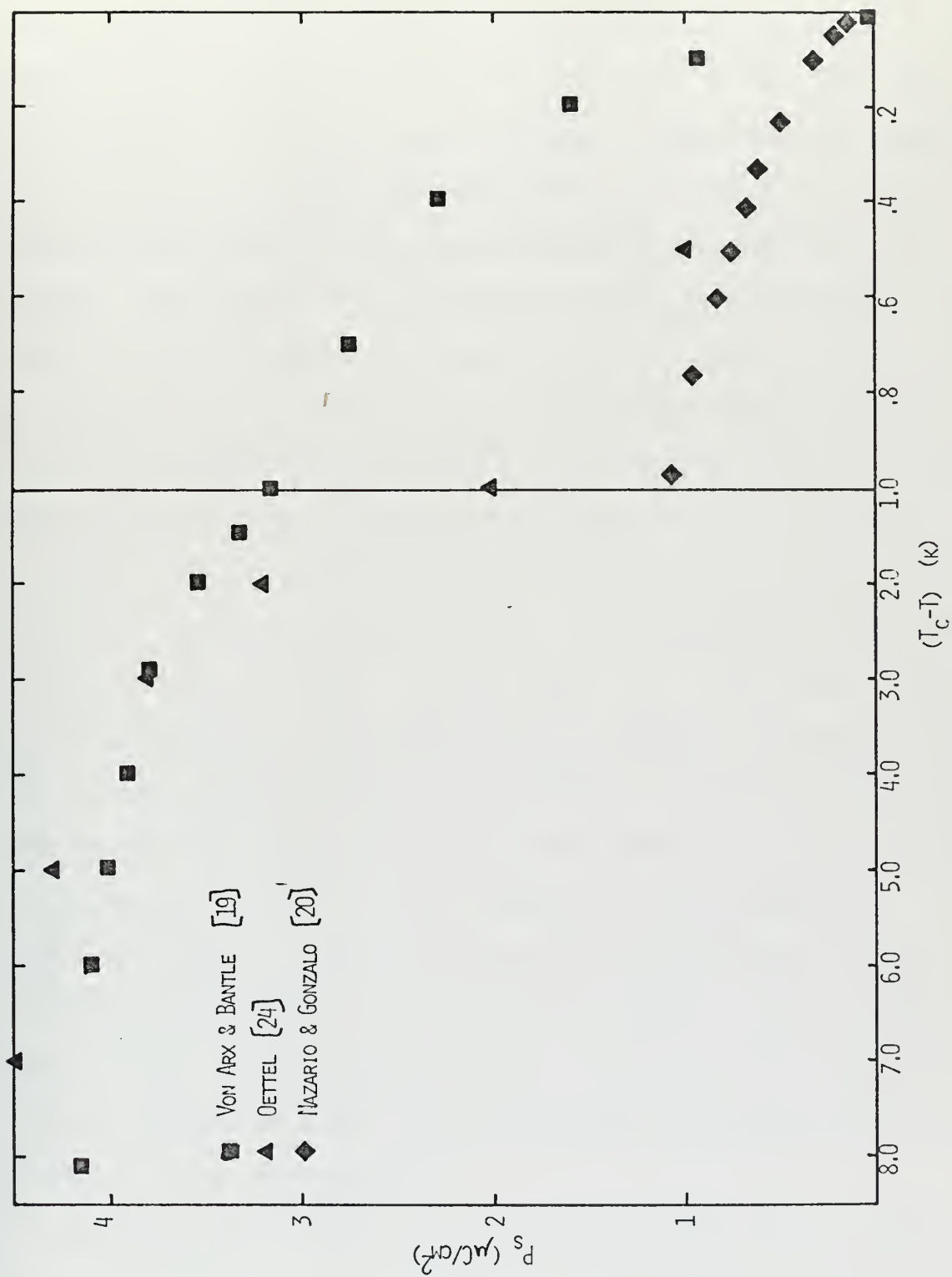


FIGURE 3. SOME SPONTANEOUS POLARIZATION MEASUREMENTS IN K_{12}PO_4

of those with the opposite polarity, until a field is reached where the crystal is a single domain aligned with the field. If the field is reduced and then reversed domains of the opposite polarity grow until the crystal is again a single domain aligned with the field. The surface charge density on the faces is directly proportional to the net macroscopic polarization of the crystal. The circuit shown in Figure 4 uses these properties to measure the polarization as a function of the applied field. An AC voltage is applied to the series combination of the capacitor, C_0 , and the sample, which has electrodes evaporated onto it to make good electrical contact and prevent spurious capacitance due to air gaps. The charge flowing from the sample is collected on the capacitor, hence the voltage across it is proportional to P . The voltage across the sample is proportional to E . If these voltages are displayed on an oscilloscope or X-Y recorder, a hysteresis loop such as that shown in Figure 5 is obtained. The area inside the loop is the work required to reverse the domains. As was pointed out in Chapter II, if a crystal remained a single domain, no hysteresis would be observed and the polarization would reverse discontinuously at $E = 0$ as required by Maxwell's rule of equal areas. We can now see another reason for this; if the crystal is a single domain, we do no work in reversing the polarization and so there can be no hysteresis.

The spontaneous polarization is usually taken to be P_0 , the linear extrapolation from the saturated portion of the curve to the P -axis at $E = 0$. P_r is called the remanent polarization and E_c

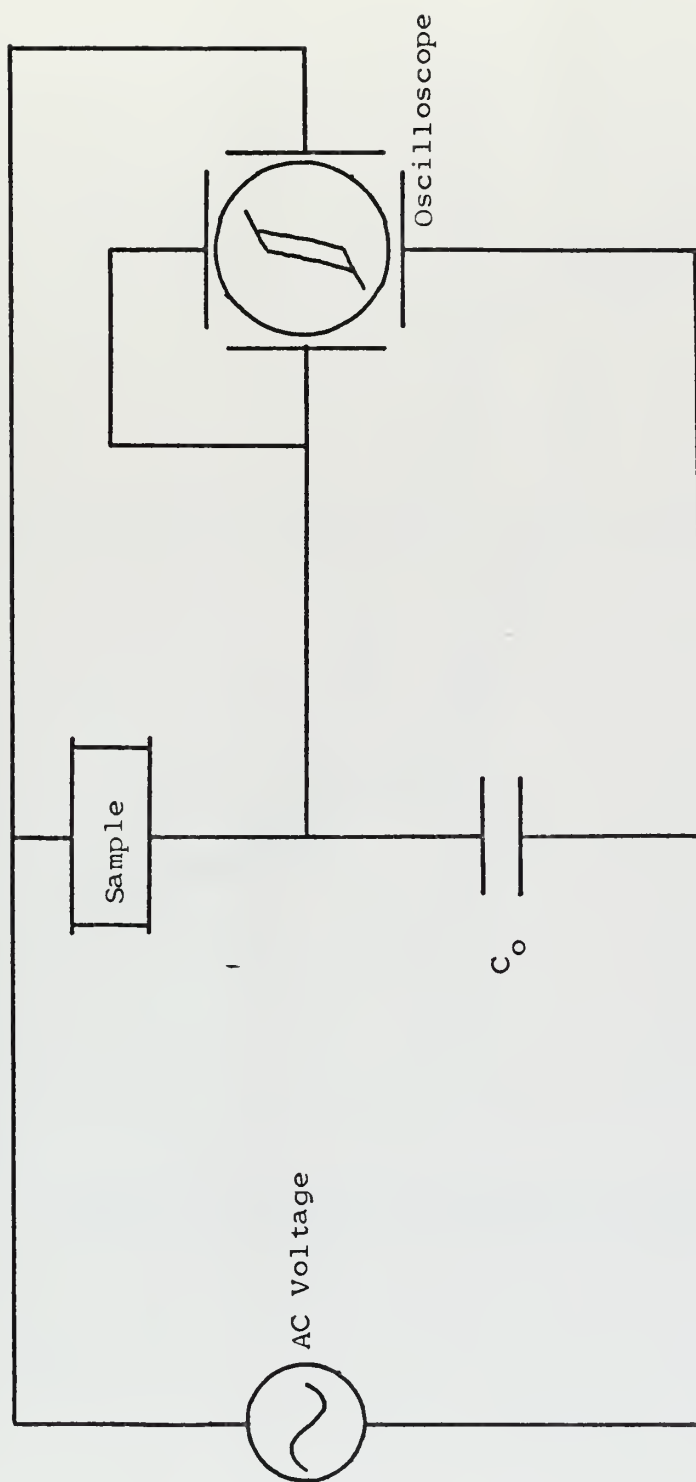


Figure 4. Sawyer-Tower Circuit for Measuring the Spontaneous Polarization

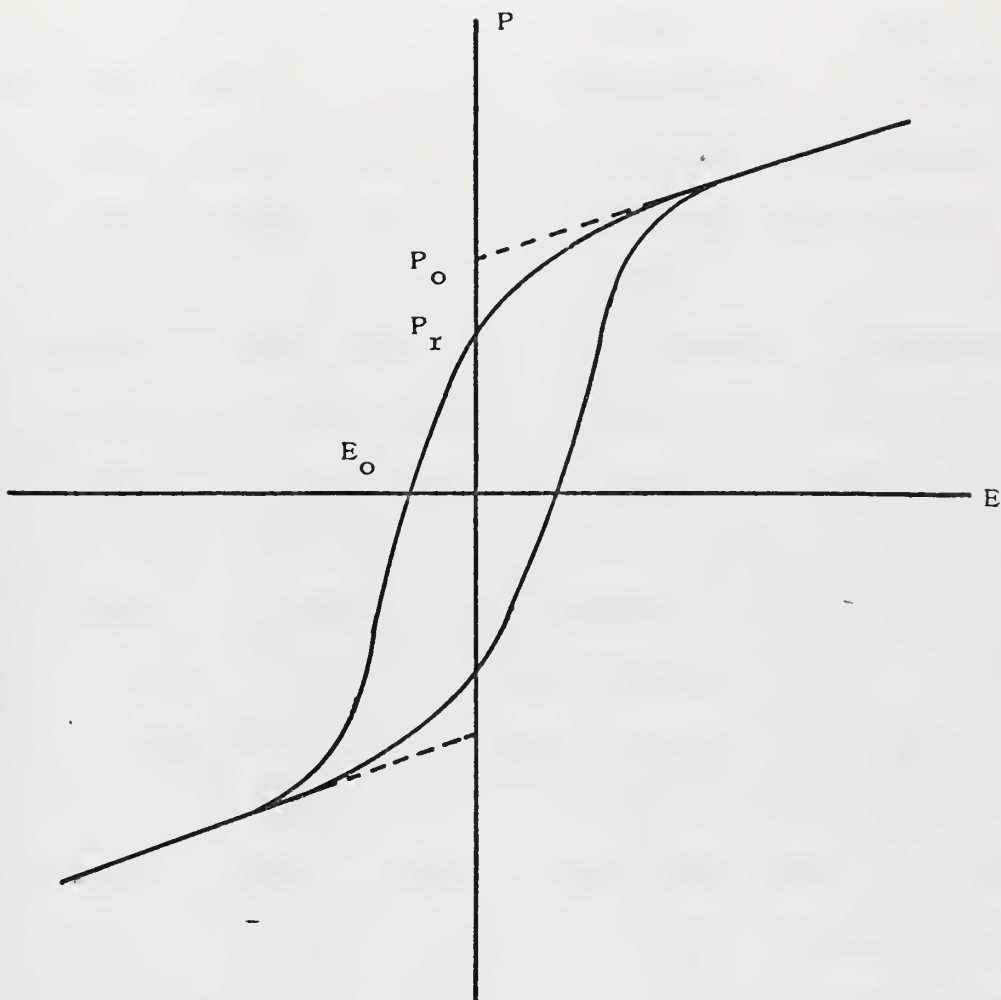


Figure 5. A Typical Ferroelectric Hysteresis Loop

the coercive field. In the temperature region very near to T_c , the relation between E and P becomes very non-linear, as was shown in Chapter II (see Figure 2). Under these conditions, the linearly extrapolated value, P_o , is larger than the actual spontaneous polarization. The remanent polarization, P_r , is smaller than P_s because part of the "roll-off" of P for small applied fields is due to domain reversal. In KDP, the domain mobility is quite large near T_c . Gonzalo observes this and notes that the loops in KDP are "less rectangular than in other ferroelectrics". In the measurements being reported in this thesis, we found that domain reversal started at about 300 v/cm on the saturated portion of the loop (see Chapter IV). The result of these considerations is that in KDP, the extrapolation procedure to find P_s from dielectric hysteresis loops is not well defined near T_c .

In the temperature region between T_c and T_2 (see Chapter II) where there is no spontaneous polarization, the non-linearity between E and P can be erroneously interpreted to give a non-zero value for P_s . This will cause an error in the determination of T_c , as well as making the transition appear to be more nearly second order. Referring to Figure 2 in Chapter II, it can be seen that, in the case of a single domain crystal, the field induced spontaneous polarization between T_c and T_2 cannot be distinguished from a spontaneous polarization below T_c . Thus it is impossible, from hysteresis measurements alone, to correctly determine T_c . In a real KDP crystal, the domain mobility is very high in this region and the crystal is able to switch polarity almost as a

single domain. Due to the above consideration, any spontaneous polarization measurements obtained from hysteresis loop measurements should be regarded with a great deal of distrust in the temperature region close to T_c .

For temperatures several degrees or more away from T_c , hysteresis loops provide fairly accurate measurements of P_s provided that the loop is traversed slowly enough. At frequencies above about 0.05 Hz, the loop is traversed in a time shorter than the thermal relaxation time between the sample and its environment, so the measurement becomes adiabatic rather than isothermal. Under these conditions, the application of an electric field causes an electrocaloric temperature increase, and the sample temperature is no longer the same as the measured temperature of the bath. In fact, the sample temperature oscillates in proportion to the magnitude of the applied field, and it is impossible to unambiguously assign a temperature to the polarization measured under these conditions. As an approximation, one can compute the average temperature change, corresponding to the rms value of the applied field, according to Equation (38a) in Chapter II. This, however, involves a prior knowledge of $(\partial P / \partial T)_E$ which is the derivative of the quantity to be measured. A further problem is that fast loops do not allow time for complete domain alignment. As discussed in Chapter IV, we found in our investigations that up to 10 minutes was required for complete domain alignment. This means the

apparent spontaneous polarization will be smaller than P_s . In short, hysteresis loop measurements of P_s must be made slowly to be of any value and should not be used close too T_c in any case.

The results of dielectric hysteresis loop measurements of P_s in KDP are shown in Figure 6. The measurements of von Arx and Bantle were made at 0.03 Hz, with care taken to avoid electrocaloric effects, using linear extrapolation to find P_s . Gonzalo's measurements were made at 60 Hz with no electrocaloric correction. He used P_r as the spontaneous polarization and located T_c by extrapolating a plot of P_s^2 vs T to the T -axis. Oettel's measurements were made by applying an electric field slowly, and optically ensuring complete domain alignment. The polarization he reports is not the spontaneous polarization but the polarization at the field necessary to obtain complete domain alignment.

Oettel's results are too high because of the presence of the aligning field. The presence of the field also changes the details close to T_c and thus his results overall are not to be relied upon. Gonzalo's measurements are far too small, primarily due to his choice of extrapolation technique. In addition, the lack of any correction for the electrocaloric effect makes his measurements practically useless. The results of von Arx and Bantle are the commonly accepted ones even though the measurements were made in 1943. They seem to have been made carefully and should be reliable, except in the region with 3K of T_c . It should be noted that all these measurements show P_s going to zero continuously at T_c indicating a second order transition.

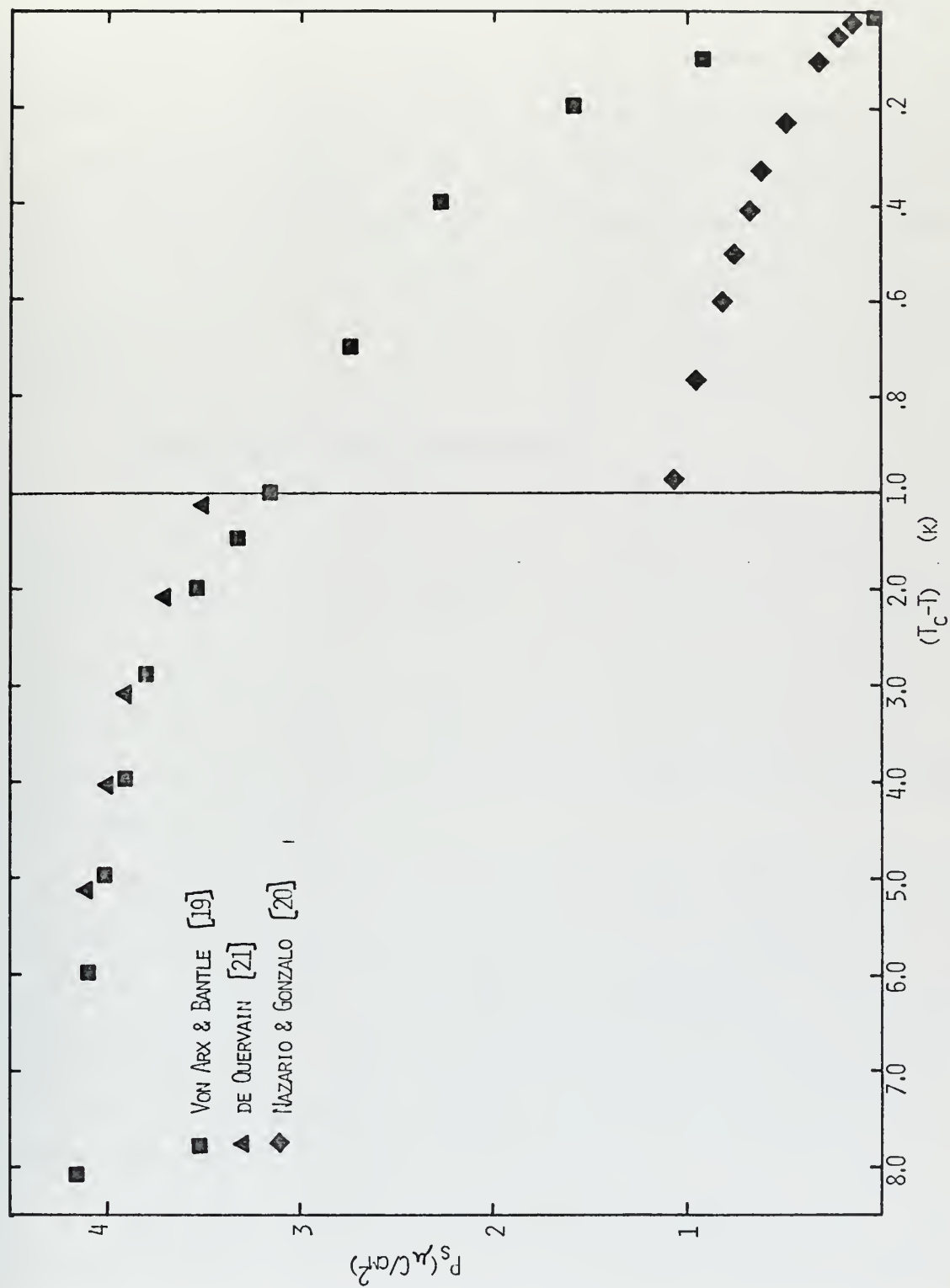


FIGURE 6. DIELECTRIC HYSTERESIS LOOP MEASUREMENTS OF P_s IN KH_2PO_4

B. INDIRECT MEASUREMENTS OF P_s IN KDP

In Chapter II we pointed out that the polarization is directly proportional to the spontaneous strain via the piezoelectric strain constant, b . This allows P_s to be calculated from measurements of x_s . Electro-optic measurements allow another indirect measurement of P_s . KDP is birefringent, the birefringence being proportional to the shear strain. Measurements of birefringence as a function of applied field (called the electro-optic effect) thus allow the calculation of P_s . These two techniques are discussed below.

1. Spontaneous Strain Measurements

For zero stress above T_c , the strain and applied field are related by $x = dE$. The strain and polarization are related by $x = bP = (d/\chi^{X=0})P$, so $b = d/\chi^{X=0}$. Both d and $\chi^{X=0}$ are known to follow a Curie law above T_c and so b is very nearly constant. If we assume that b remains constant into the ferroelectric phase, then measurements of d and $\chi^{X=0}$ above T_c coupled with measurements of x_s below T_c give P_s .

Von Arx and Bantle [23] have measured the strain in KDP as a function of field above and below T_c . The technique was to measure the elongation of the sample perpendicular to the c -axis interferometrically. From the measurements above T_c they found the temperature dependence of d and using the values of χ^X obtained by Busch [24] they calculated b .

Below T_c , they observed hysteresis between x and E . This is to be expected since the strain in adjacent domains is opposed

as is the polarization. Using the linear extrapolation technique, they obtained x_s from the hysteresis loops and using their value for b , calculated P_s . The results are nearly identical to their dielectric hysteresis measurements of P_s .

They also measured the spontaneous strain with no applied field which is due to a small quadratic term in the free energy, which we have omitted. (This term also gives rise to electrostriction.) They found that for a shorted crystal they could not obtain reproducible results, but for an open circuited crystal they obtained agreement with their hysteresis measurements. In an open circuited crystal the electrical boundary conditions are not defined since any remanent polarization will collect neutralizing surface charges giving rise to an effective field in the sample. It is the lack of reproducibility of the remanent polarization which probably caused the inconsistency in their results with a shorted crystal.

The objections to this method as one for measuring P_s close to T_c are the same as for dielectric hysteresis loops. The non-linearities between E and x make it impossible to locate T_c accurately or to make an unambiguous extrapolation to find x_s . If the problem of the remanent polarization could be solved, the quadratic effect with well defined electrical boundary conditions would be a good measure of P_s , but the capricious behavior of domains prevents this.

De Quervain [25] has measured the spontaneous strain below T_c , without any external applied field, by means of X-ray diffraction. His measurements are independent of domains, electrical boundary conditions, or non-linearities between E and x , depending only on the microscopic deformation of the crystal unit cell. Comparing his value for x_s at 110K with von Arx and Bantle's value for P_s at that temperature, he calculates $b = \frac{x_s}{P_s}$ and uses this value for b to compute P_s for the rest of his data. He also compares his value for b with that calculated from von Arx and Bantle's data above T_c and shows that b is, in fact, nearly constant.

The results of these spontaneous strain measurements are shown in Figure 7 along with von Arx and Bantle's dielectric hysteresis measurements for comparison. De Quervain's results are free from any serious objections and are the most accurate determination of x_s made so far. It should be noted that, to obtain spontaneous polarization measurements from them, one needs a reference polarization from which to calculate b . If some value other than von Arx and Bantle's were preferred, De Quervain's results could be linearly adjusted to fit it. It should also be noticed that De Quervain's results diverge from those of von Arx and Bantle near T_c , with De Quervain's indicating the possibility that the transition may be more nearly first order.

2. Electro-optic Measurements

According to Pockles [26], the transverse birefringance, $\Delta\eta$, for KDP is:

$$\Delta\eta = \eta_3 - \eta_1' \approx (\eta_3 - \eta_1) + \frac{1}{2} \eta_1^3 f_{63} E_z^2,$$

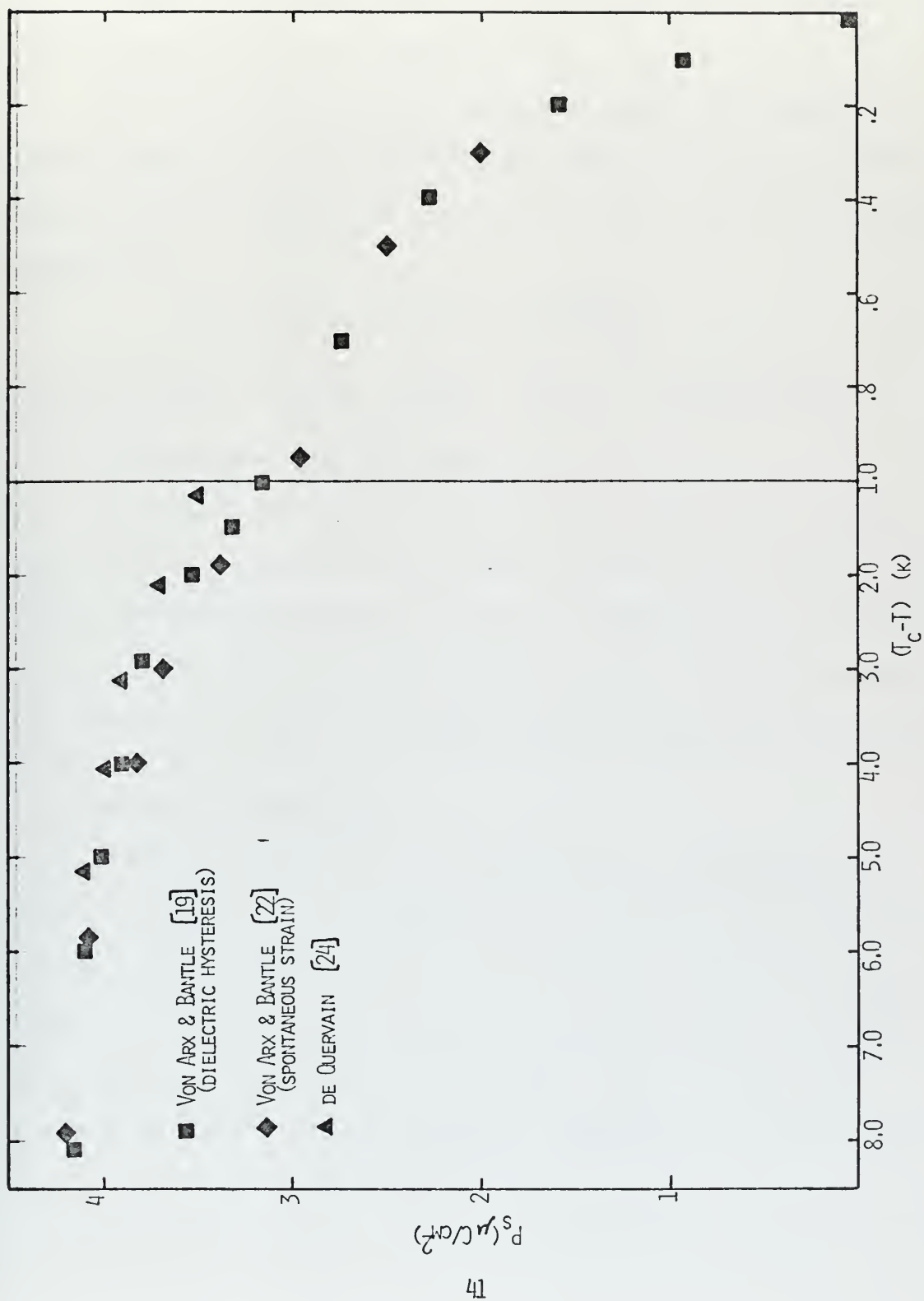


FIGURE 7. SPONTANEOUS POLARIZATION AS CALCULATED FROM THE SPONTANEOUS STRAIN IN KH_2PO_4

where the primed refractive indices refer to the orthorhombic crystal axes and the unprimed to the tetragonal crystal axes. f_{63} is called the electro-optic coefficient.

This equation indicates that the change in birefringance is proportional to the applied field. Experimentally it is found that f_{63} follows a Curie law above T_c , so that $f_{63}/\chi^{X=0}$ is constant. We then have:

$$\Delta\eta = (\eta_3 - \eta_1) + \frac{1}{2} \eta_1^3 (f_{63}/\chi^{X=0}) P_z.$$

Assuming $f_{63}/\chi^{X=0}$ remains constant below T_c , we can calculate P_s from the spontaneous birefringance $\Delta\eta_s$.

Swicker and Scheerer [27] have made electro-optic measurements in KDP and deuterated KDP above and below T_c . Below T_c they obtained hysteresis between $\Delta\eta$ and E , as expected, since $\Delta\eta$ depends on the strain. Again, the method of extrapolation and location of T_c are problems. They do not report their results for P_s in KDP.

C. PYROELECTRIC TECHNIQUES

Since the polarization of a ferroelectric is temperature dependent, a change in the temperature of a crystal, ΔT , will cause a change in the polarization, ΔP . The charge released from the surface of the crystal during the temperature change is directly proportional to the polarization change. This is called the pyroelectric effect. The pyroelectric coefficient is defined as:

$$\emptyset \equiv dP/dT.$$

In a real crystal with no electric field applied, the macroscopic polarization is:

$$P_r = (2f-1)P_s,$$

where f is the fraction of domains aligned with the remanence.

Assuming that f does not change for small changes ΔT , then:

$$\emptyset = (2f-1)\emptyset_s,$$

where $\emptyset_s = dP_s/dT$. If f can be considered to be independent of temperature, measurements of \emptyset as a function of temperature allow the calculation of P_s as follows:

$$P = \int \emptyset dT = \int (2f-1)\emptyset_s dT = (2f-1) \int \emptyset_s dT = (2f-1)P_s.$$

This equation indicates that the P calculated from measurements of \emptyset is a constant times P_s . Thus, if an independent measurement of P_s (by hysteresis loops for example) is available, such data can be normalized to that point so as to obtain P_s from measurements of \emptyset .

Chynoweth [28] has used such a technique to measure P_s in Barium titanate and triglycene sulfate (TGS). He measures the current flowing from a sample when it has been heated by a light pulse. The current is:

$$i = (\partial P / \partial T)(dT/dt) = \emptyset(dT/dt).$$

He finds that the initial heating rate, $(dT/dt)_0$ times the specific heat at zero applied field is constant, so that $\emptyset = (\text{const})(i_0)$ ($C_E = 0$), where i_0 is the initial current and $C_E = 0$ is the specific heat. Using the results of a hysteresis loop measurement of P_s at

one point he integrates to find P_s for the rest of the temperature range covered in his measurements. The results he obtains in this fashion compare very well with the results obtained from dielectric hysteresis measurements in BaTiO_3 and TGS. As has been pointed out, however, the square hysteresis loops obtained in these materials indicate that the domain mobility is low and that, after poling of the sample, the remanent polarization is consistent and f is very nearly one.

In our investigations on KDP, we found that the remanent polarization decreases in magnitude markedly as T_c is approached. The results were not reproducible even after the application of an aligning field. We also noted that the time required for complete domain alignment, after application of a field, decreased as T_c was approached. These considerations all lead to the conclusion that, in KDP, f is temperature dependent and cannot be taken outside the above integral. Thus, the pyroelectric effect, without the use of an applied aligning field, is not suitable as a method for measuring P_s . It should also be noted that Chynoweth has reported the results of his method for a great variety of ferroelectrics, but KDP is not among them.

An alternate approach is the application of an aligning field, making $f = 1$. If the measurements of \emptyset made under these conditions can be corrected for the presence of the field, one can obtain P_s . Azoulay et.al. [29] have used this technique to measure P_s in KDP. They applied a large, DC field to the sample below T_c and

simultaneously observed the small signal, AC susceptibility to ensure saturation of the polarization. They then heat the sample rapidly through the transition with the DC field applied, measuring the charge which flows from the sample. They then measure the small signal, AC susceptibility above the transition and remove the DC field.

They attempt to correct for the presence of the field during the measurement by assuming that, below T_c , the polarization is $P_B = P_s + \chi_B E$ and above T_c it is $P_A = \chi_A E$. They thus obtain:

$$P_s = (P_B - P_A) + (\chi_A - \chi_B)E.$$

The assumption in this correction is that the susceptibility is linear (i.e. P and E are linearly related) and that it has only two values, one above T_c and one below, neglecting its temperature dependence. For temperatures well above or below T_c , χ is reasonably linear. For temperatures well below T_c , the value of P_s obtained at the initial temperature by this method is reasonably accurate. The data for all points other than the initial point cannot be used since the simple correction used does not account for the temperature dependence of χ , nor for the non-linearity close to T_c .

This technique using only the initial point as a data point could be used for temperature well below T_c . It could not be used close to T_c however due to the non-linearity of χ in that region.

D. ELECTROCALORIC TECHNIQUES

All the methods discussed so far are isothermal. If the measurements are made adiabatically, the electrocaloric effect can be

utilized. In Chapter II it was shown that the electrocaloric temperature change and polarization change due to the adiabatic application of an electric field are related by:

$$\Delta T = (T/C_p)(\partial E/\partial T)_P \Delta P.$$

If the validity of Landau theory in describing the ferroelectric phase transition is assumed, we obtain:

$$\Delta T = (\alpha T/2C_p) \Delta(P^2).$$

If we take $\Delta T = 0$ for no applied field (sample shorted), then below T_c :

$$\Delta T = (\alpha T/2C_p)(P^2 - P_s^2),$$

which says that a plot of ΔT vs P^2 should allow a linear extrapolation to P_s^2 at $\Delta T = 0$. Above T_c :

$$\Delta T = (\alpha T/2C_p)P^2,$$

and P^2 should extrapolate to zero at $\Delta T = 0$. If the assumption holds, the non-linearity between E and P does not affect measurements made in this manner.

A schematic diagram of the apparatus used to make electrocaloric measurements is shown in Figure 8. The operation is basically that of an adiabatic, DC Sawyer-Tower circuit. The sample is taken around an adiabatic hysteresis loop, step-by-step. At each point the sample temperature, series capacitor voltage, and applied voltage are recorded. ΔT is the difference between the temperature at a point and the temperature at zero applied voltage. P is proportional to the series capacitor voltage. Thus a plot of P^2 vs ΔT can be obtained.

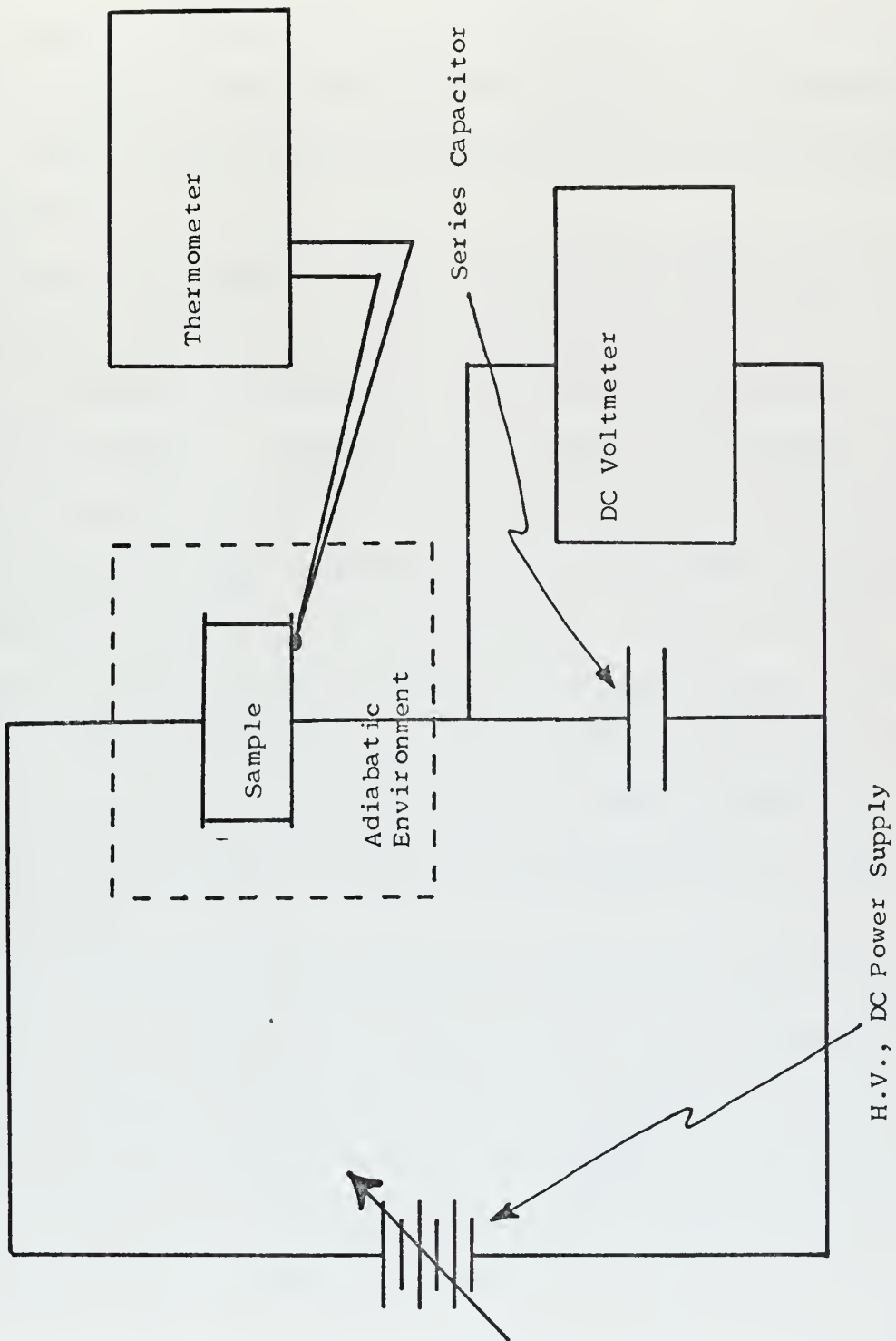


Figure 8. Schematic Diagram of the Electrocaloric Apparatus for Making Polarization Measurements

The polarization measured is the macroscopic polarization of the sample. Thus, the effect of domains is to make P and thus P^2 smaller than the actual polarization in the sample for small values of the applied voltage. This will make the ΔT vs P^2 data "round-off" for small ΔT rather than follow a straight line down to the axis. Hence P_s^2 must be extrapolated from the saturated portion of the data.

Wiseman and Kuebler have used this technique for measurements on Rochelle salt [30] and Strukov has used it for TGS [31]. Their results compared with dielectric hysteresis measurements are shown in Figures 9 and 10. Although their results are consistent with previous measurements, the technique rests on the assumption that Landau theory is valid. Neither of their measurements test the thermodynamic consistency of their results. Such a test is accessible from the data available in such measurements. As was shown in Chapter II, the ΔE vs ΔT data allow an independent calculation of P_s which can be used to check the thermodynamic consistency of the results as well as the assumption that Landau theory holds.

Since electrocaloric measurements seem to take better account of all effects and are least ambiguous near T_c , it was decided to use this technique to measure P_s near T_c in KDP, and to try to obtain a check on the thermodynamic consistency of the method and on the assumptions. The next chapter deals with the particulars of the experimental techniques used.

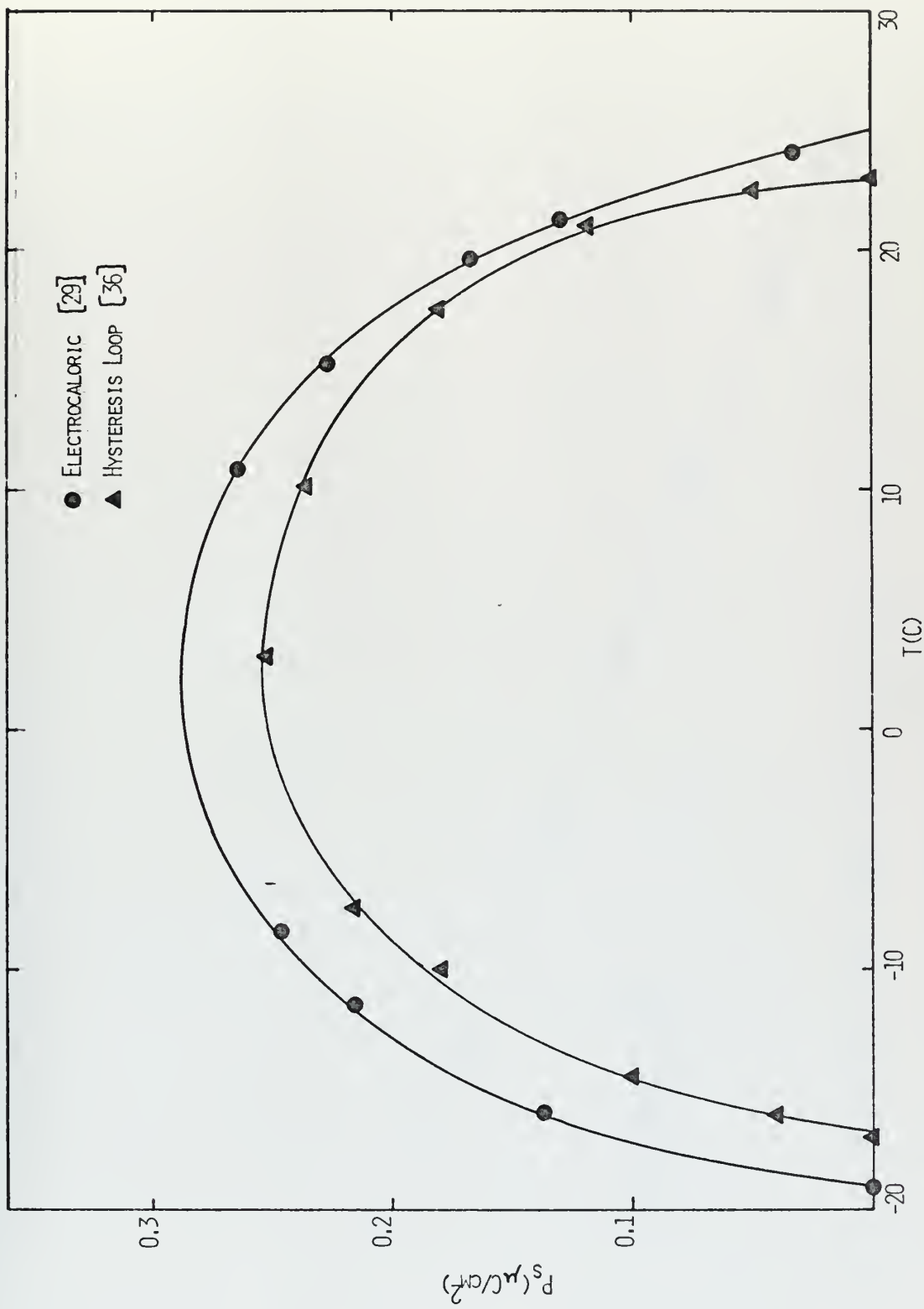


FIGURE 9. MEASUREMENTS OF P_s IN ROCHELLE SALT

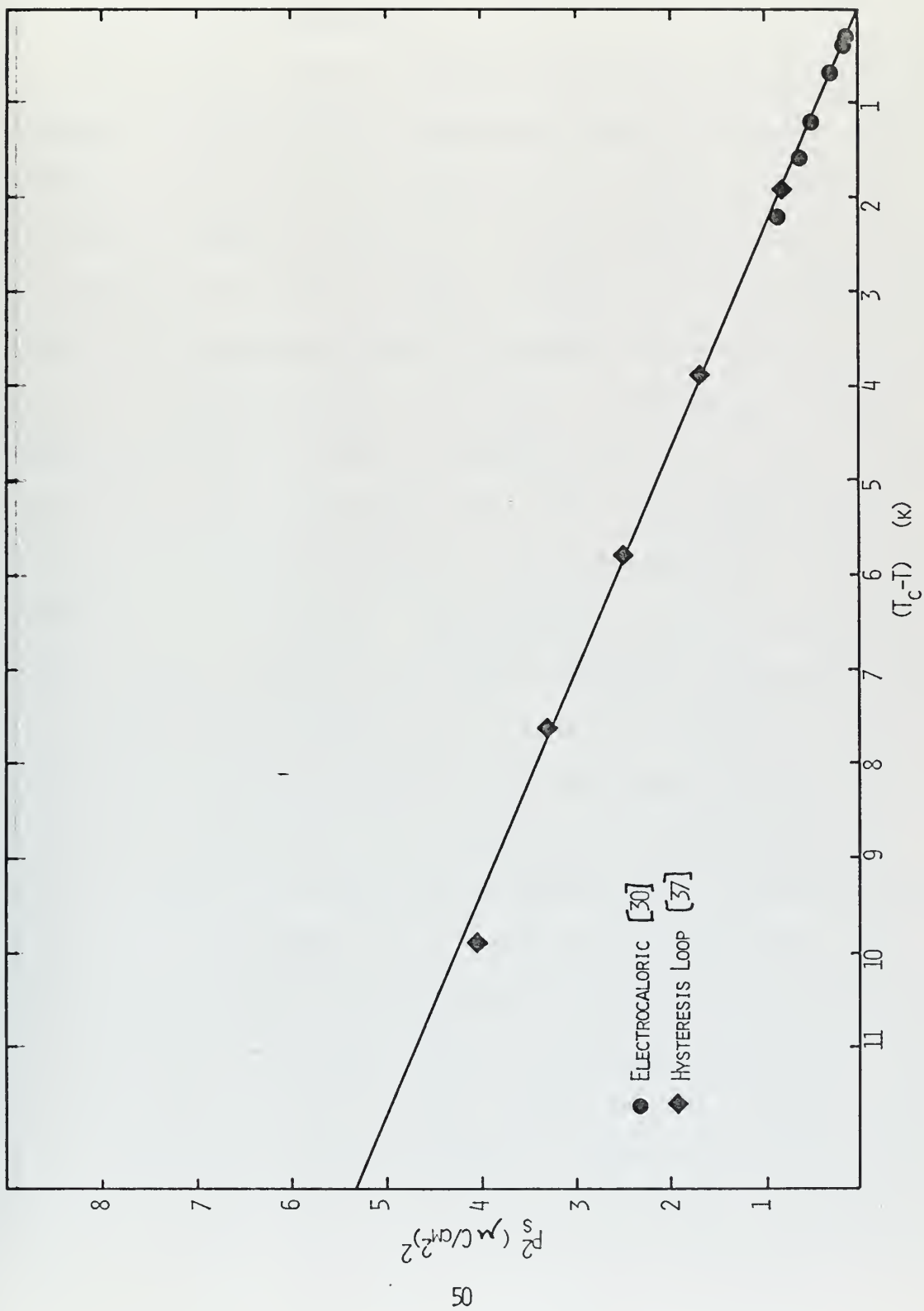


FIGURE 10. MEASUREMENTS OF P_s^2 IN TRIGLYCINE SULFATE

IV. EXPERIMENTAL EQUIPMENT AND PROCEDURES

A. CRYOSTAT AND THERMOMETRY

The adiabatic sample environment consisted of a cryostat designed to operate in the temperature range 80 - 150K. A schematic diagram of its configuration is shown in Figure 11. The sample chamber, consisting of three concentric copper cans, is suspended in a bath of liquid nitrogen by a thin walled stainless steel tube which served as a conduit for the electrical leads and as a vacuum connection. The outer can served as a vacuum chamber and was evacuated to approximately 5×10^{-6} torr. The center can, called the shield, had evenly distributed bifilar heaters wound on it and its lid, and was maintained at the same temperature as the sample. The inner can acted as a radiation shield between the shield and sample, which was suspended inside it, by three nylon threads. The shield was maintained at the same temperature as the sample by the circuit shown in Figure 12. The temperature difference between the shield and the sample was sensed by means of a differential thermocouple, one junction of which was on the sample and the other on the shield lid. The thermocouple voltage was detected by a Keithly 148 nanovoltmeter. The amplified error signal from the nanovoltmeter recorder output served as the input to a current controller which regulated the power to the shield and lid heaters so that it just balanced the heat lost by conduction and radiation to the outer can, which was

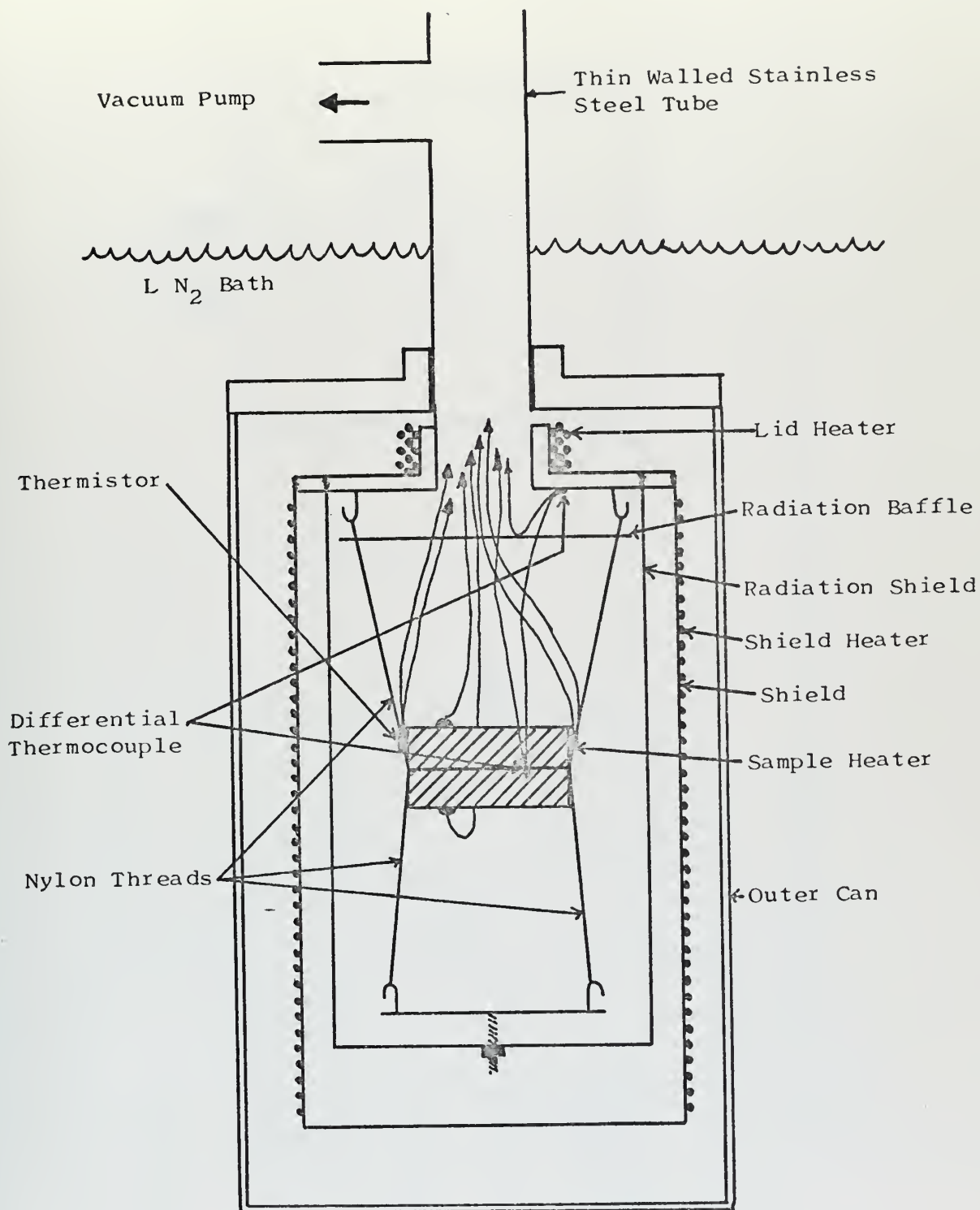


Figure 11. Detailed Schematic Diagram of the Adiabatic Sample Chamber

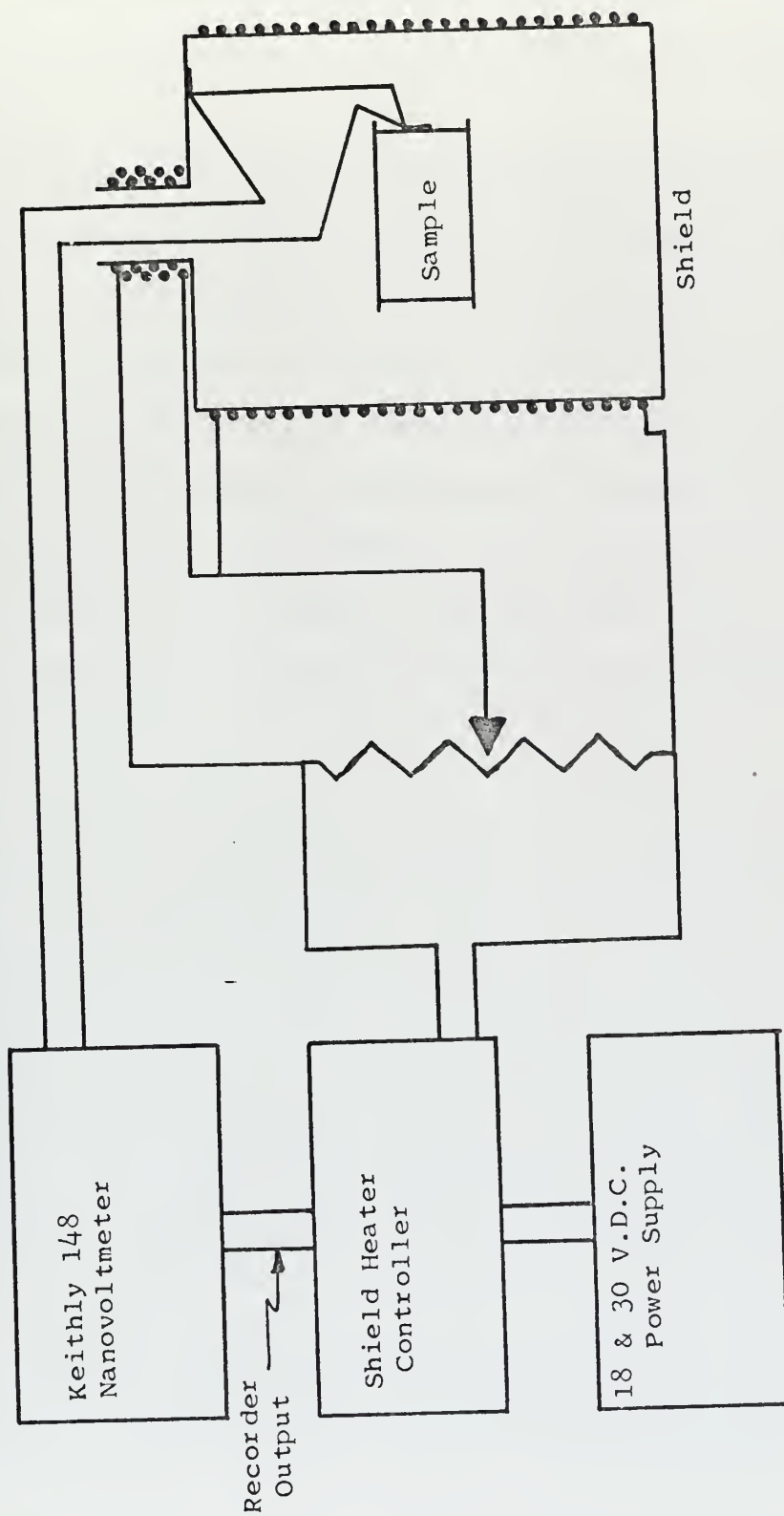


Figure 12. Schematic Diagram of the Adiabatic Thermostat

at liquid nitrogen temperature, thus keeping the sample and shield at the same temperature. The current controller employed a combination of proportional and reset control using operational amplifiers.

The output of the current controller was divided so that the ratio of power between the shield and lid heaters could be adjusted to minimize thermal gradients in the shield. The gradients could not be entirely eliminated and so the temperature difference sensed by the differential thermocouple was not the same as the average temperature difference between the sample and shield. This was compensated for by varying the zero suppress control on the nanovoltmeter, offsetting the null position, until no thermal drift of the sample could be observed by monitoring the sample temperatures.

In operation, the nanovoltmeter was set for 100 μ v full scale sensitivity. The maximum deviations from null were 0.2 μ v or 10^{-3} K. The average deviation was about one tenth of this. The thermal drift of the sample could be kept to less than 10^{-4} K/hr by careful adjustment of the nanovoltmeter zero suppress. The response of the system was such that the shield temperature continued to match that of the sample through rapid electrocaloric temperature changes of 0.05 K with no noticeable deflection on the nanovoltmeter.

The sample temperature was measured by means of a thermistor, glued to the sample. Its resistance was measured by a low power,

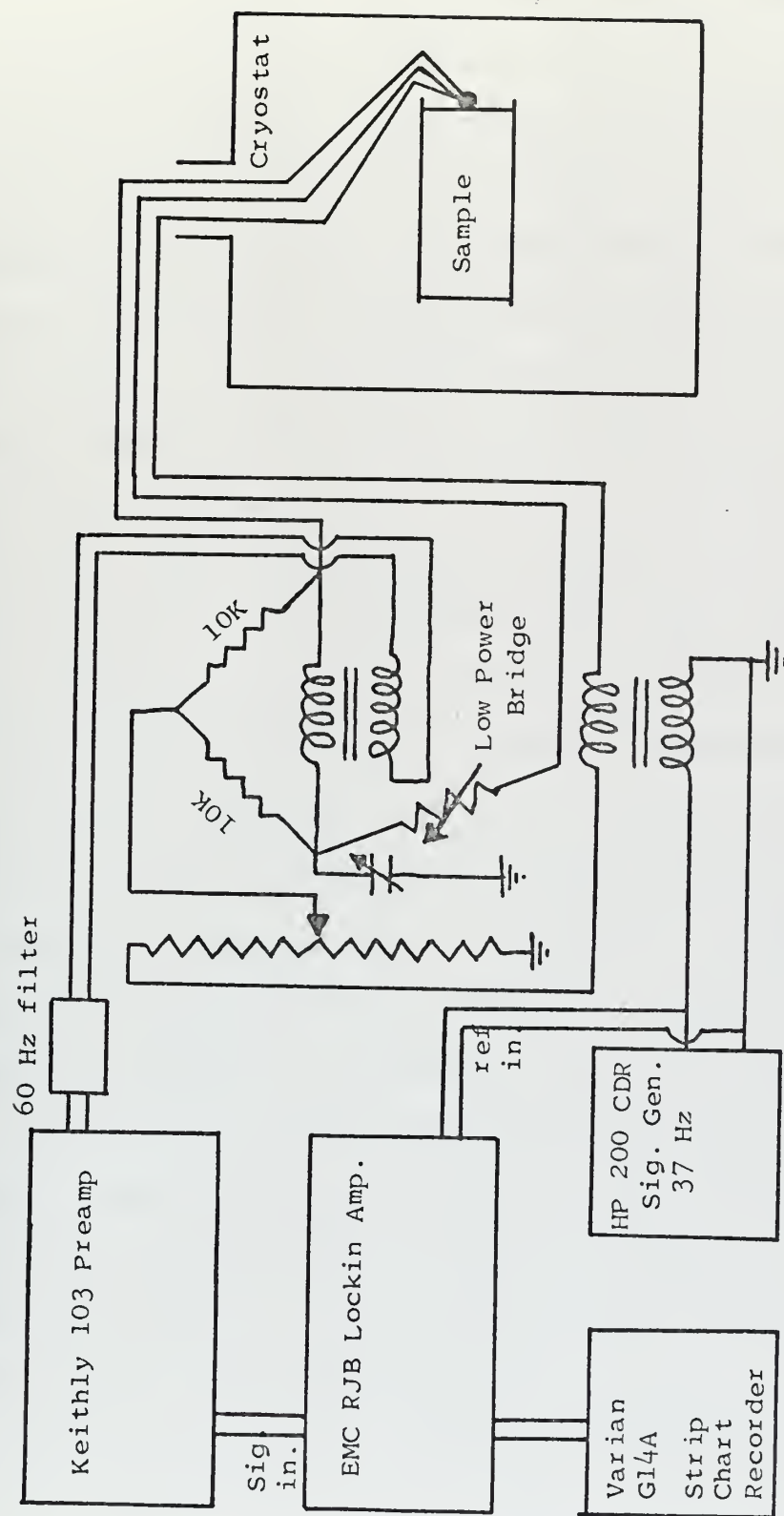


Figure 13. Schematic Diagram of Temperature Measuring Apparatus

AC bridge employing a lock-in amplifier as a null detector.

Figure 13 is a schematic diagram of the equipment employed.

The thermistor was type RL10X04 manufactured by Keystone Carbon Company which had a resistance of approximately 1500 ohms at 122K. It was connected to the bridge in a three lead configuration so that changes in the lead resistance caused by temperature variations were evenly distributed and did not affect the bridge balance. The system was operated at 37 Hz to avoid 60 Hz pick-up. The power dissipated in the sample due to joule heating of the thermistor was 3×10^{-8} watts and caused negligible heating. At the lockin amplifier attenuations used during data accrual the resistance could be interpolated to 0.001 ohms, corresponding to 1.5×10^{-5} K in the temperature region of interest.

The system was calibrated by making simultaneous measurements, over the whole temperature range, with the thermistor and a platinum resistance thermometer, calibrated by the National Bureau of Standards. From this data, $(1/R)(dR/dT) = K$ was plotted and found to be constant over the temperature region of interest. Temperature changes were computed from $\Delta T = (1/R)(\Delta R/K)$.

Cycling the thermistor from 80K to room temperature and back usually caused a small (1 ohm) shift in the thermistor calibration which could be detected by a shift in the resistance at which the transition occurred. Since K was constant, this shift had negligible effect on measurements of ΔT .

Heating the sample was effected by means of a 100 ohm carbon resistor which was glued to the sample. Cooling was accomplished by turning off the shield power.

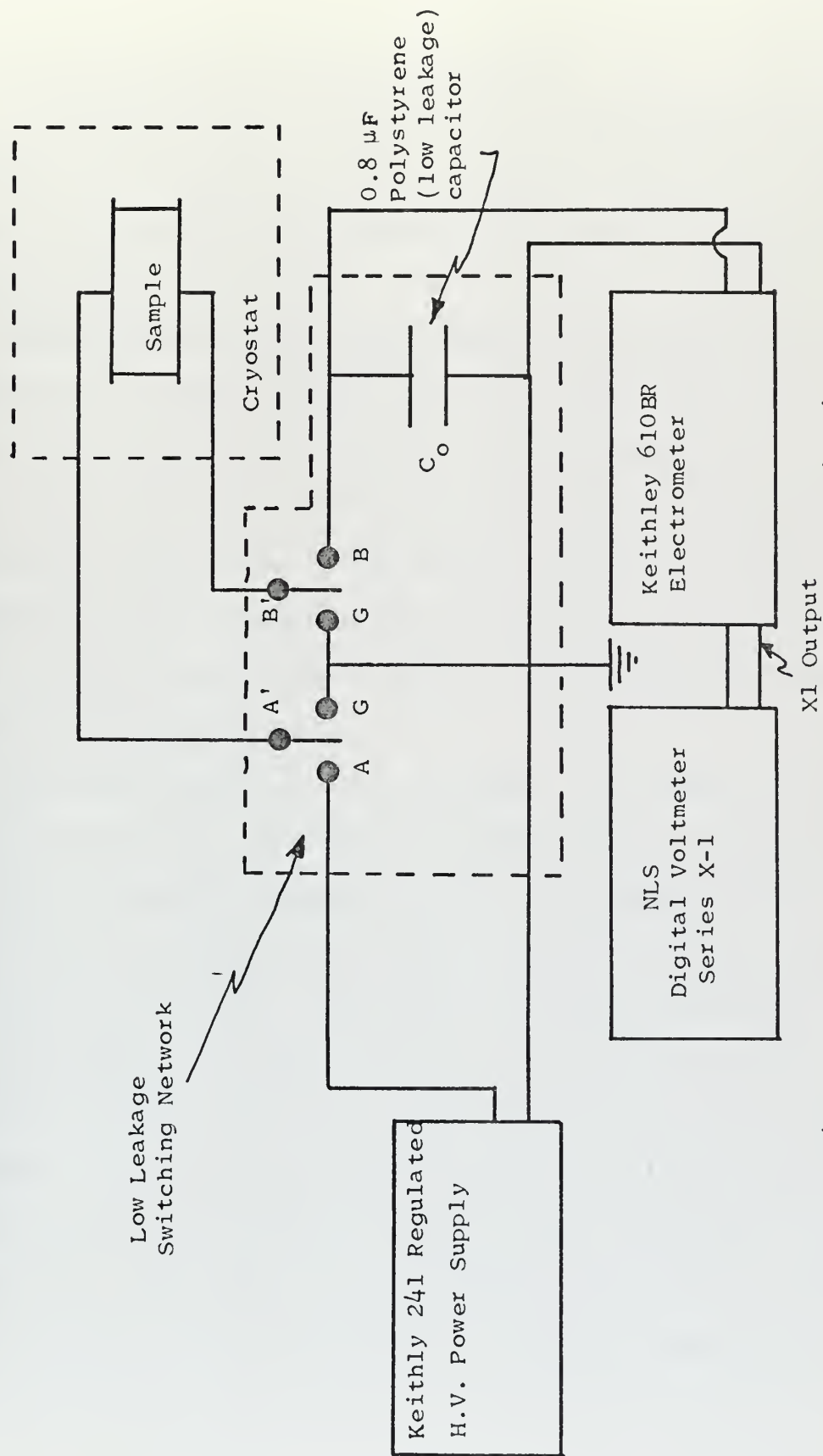


Figure 14. Schematic of Electrocaloric Measurement Circuit

B. APPARATUS FOR ELECTRICAL MEASUREMENTS

A schematic diagram of the apparatus used to measure the electrocaloric polarization changes is shown in Figure 14. Measurements were made with the two switches in the A'-A and B'-B positions.

Using the high voltage power supply, $0 - \pm 1000$ V could be applied to the series combination of the sample and capacitor, C_0 . The charge flowing from the sample due to an electrocaloric polarization change was collected on the capacitor. The capacitor voltage was measured by an electrometer because of its high input impedance. The X1 output of the electrometer served as the input to a digital voltmeter which could be read with greater precision than the electrometer scale.

The charge increments due to changes in the applied voltage were as small as 4×10^{-8} Clb., so great care was taken to eliminate paths for leakage currents. All connections were made with coaxial connections and coaxial cable, with teflon insulation, was used for all leads. The special low-leakage switching network was constructed to eliminate leakage from the high voltage side of the power supply to the high side of the capacitor. The two switches were constructed of teflon and had guarding electrodes around each of the terminals isolating them electrically from each other. The guards and all shielding were kept at ground potential. The result of these precautions was that leakage

currents were less than 10^{-14} amp. During preliminary trials before the above precautions were taken, leakage currents of 10^{-10} amp obscured any measurements.

A 0.8 μ F., polystyrene capacitor with a leakage resistance of 10^{14} ohms was used for C_0 . This was necessary to prevent measurable decay of the voltage across it which could seriously effect the polarization measurements. During initial trials a mylar capacitor with 10^{11} ohms leakage resistance was used and found to be unsatisfactory. A Keithly 610BR electrometer was used for a voltmeter because its high input impedance of 10^{14} ohms would not lower the capacitor leakage resistance. The electrometer thus served as an impedance matching device for the digital voltmeter. The overall accuracy of this system was 8×10^{-10} Clb.

C. SAMPLE PREPARATION

The configuration of a typical sample is shown in Figure 15. The samples were single crystals of KH_2PO_4 cut into thin plates, with evaporated gold or tin electrodes entirely covering the two faces perpendicular to the crystal c-axis. Electrode contact to leads was made by pressing a small piece of indium onto the electrode, putting the lead on the indium and pressing another piece of indium on top of that. To ensure good thermal contact, the thermistor and heater each had a copper tab soldered to one lead and the tab was then glued to the edge of the sample with GE7031 varnish. The nylon suspension threads were tied and glued

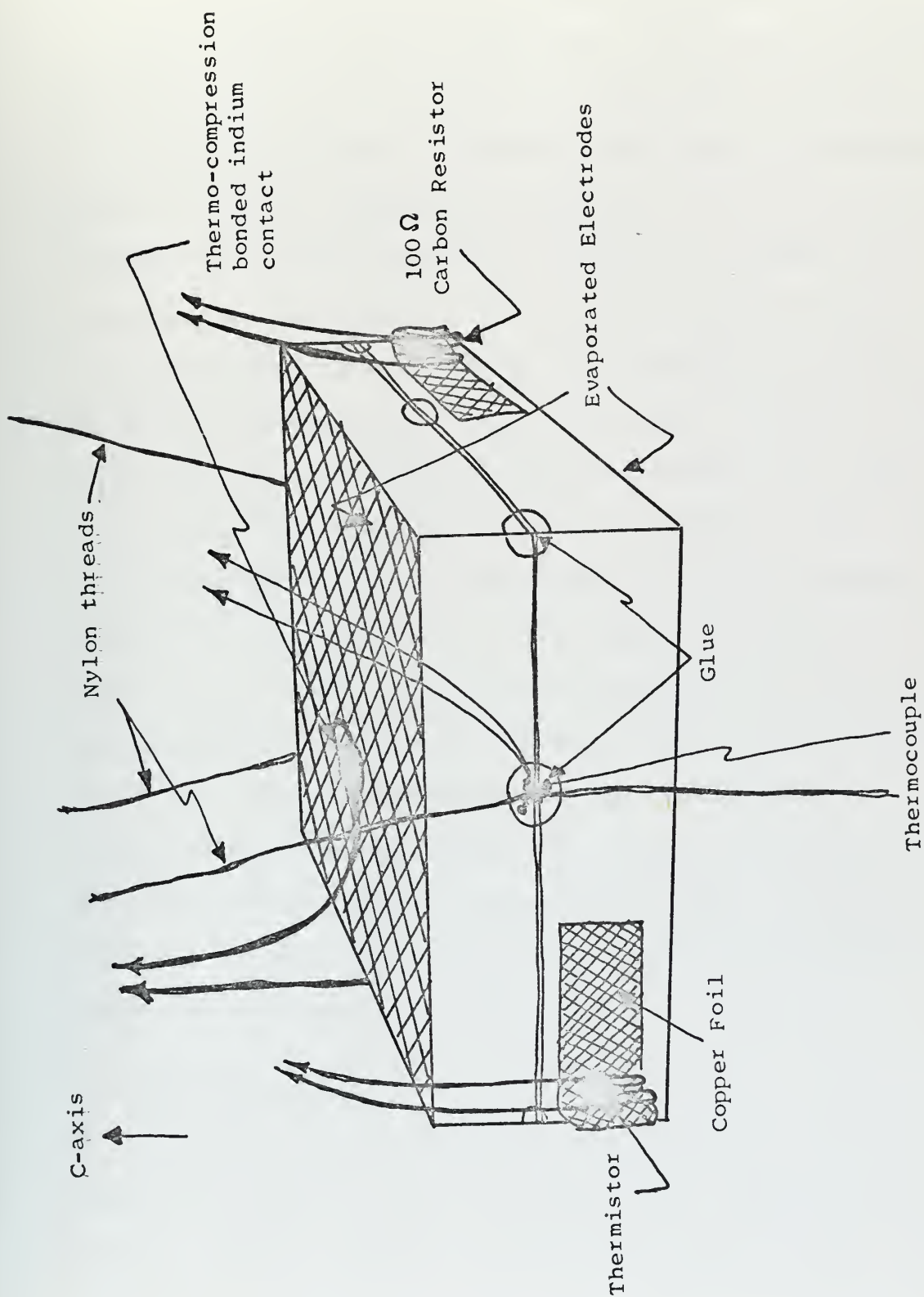


Figure 15. Typical Sample Configuration

to a cotton thread running around the edge of the sample, glued in as few places as possible to minimize clamping effects.

Three different samples were used. All three were obtained from Clevite Corporation and came on three separate orders, each at least one year apart. Presumably they came from different boules. The first sample had dimensions 2 x 2 x 0.6 cm, and had 300 \AA gold electrodes which were transparent to light so as to minimize clamping effects. This sample was used to make preliminary measurements of E vs ΔT . The resulting values for $(\partial P / \partial T)_E$ were unexpectedly small and during a subsidiary investigation into the properties of evaporated films it was found that transparent films have many small holes in them. Since it was felt that either holes or film stress effects could cause $(\partial P / \partial T)_E$ to be too small, two more samples were prepared. Both were 1" x 1" x 0.5". The first had 1500 \AA tin electrodes and the second 1500 \AA gold electrodes. Since tin has a much lower yield stress than gold, it was hoped that this would resolve the questions about the preliminary measurements. Both these samples were used to take complete electrocaloric data, and both gave identical results which also concurred with the preliminary data. (For further discussion see Chapter V.)

D. EQUIPMENT OPERATION AND DATA ACCRUAL

The basic method of operating the system was to traverse an adiabatic hysteresis loop in voltage steps, recording the capacitor voltage, applied voltage, and temperature after thermal and electrical equilibrium at each step. Preliminary measurements with

the equipment indicated that the primary factor governing the reproducibility of results was whether saturation (complete domain alignment) had been achieved. The unsaturated portions of the loop were not reproducible due to the lack of consistency in domain reversal before saturation was reached. For this reason the unsaturated portions of the loop were not investigated, reducing the amount of time necessary to traverse the loop and minimizing any possible thermal drift of the sample.

Since approximately four hours were required to traverse the hysteresis loop for each data point, any thermal drift of the sample had to be eliminated before starting to take data. This was accomplished by observing the thermistor resistance, with the sample shorted, for about an hour, adjusting the zero suppress on the nanovoltmeter until the change in temperature with time was less than 10^{-4} K/hr.

The switching network was then put into the electrocaloric position and ± 950 V applied with the power supply. The initial voltage on each leg of the loop was always a maximum in order to achieve domain alignment. It was observed that on this initial step, the voltage across the series capacitor would increase very rapidly initially and then continue to increase slowly for about 10 minutes before finally becoming steady. This indicates that it takes approximately that long for the initial domain alignment to occur. The initial thermal equilibrium took about 15 minutes. The voltage was then reduced in 100V steps, waiting for thermal and electrical equilibrium at each point. The electrical

equilibrium was usually quite rapid until voltages below $\pm 150V$ were reached because the domains were already aligned. Thermal equilibrium usually require 5-10 minutes. Following the $\pm 50V$ step, the applied voltage was set to zero. After equilibrium at zero, the power supply polarity was reversed and the process repeated, completing the loop. During the time the loop was being traversed, the sample was never shorted, even when the power supply was set on zero. This would have opened the lead to the series capacitor and all electrical reference to the already established portion of the loop would be lost.

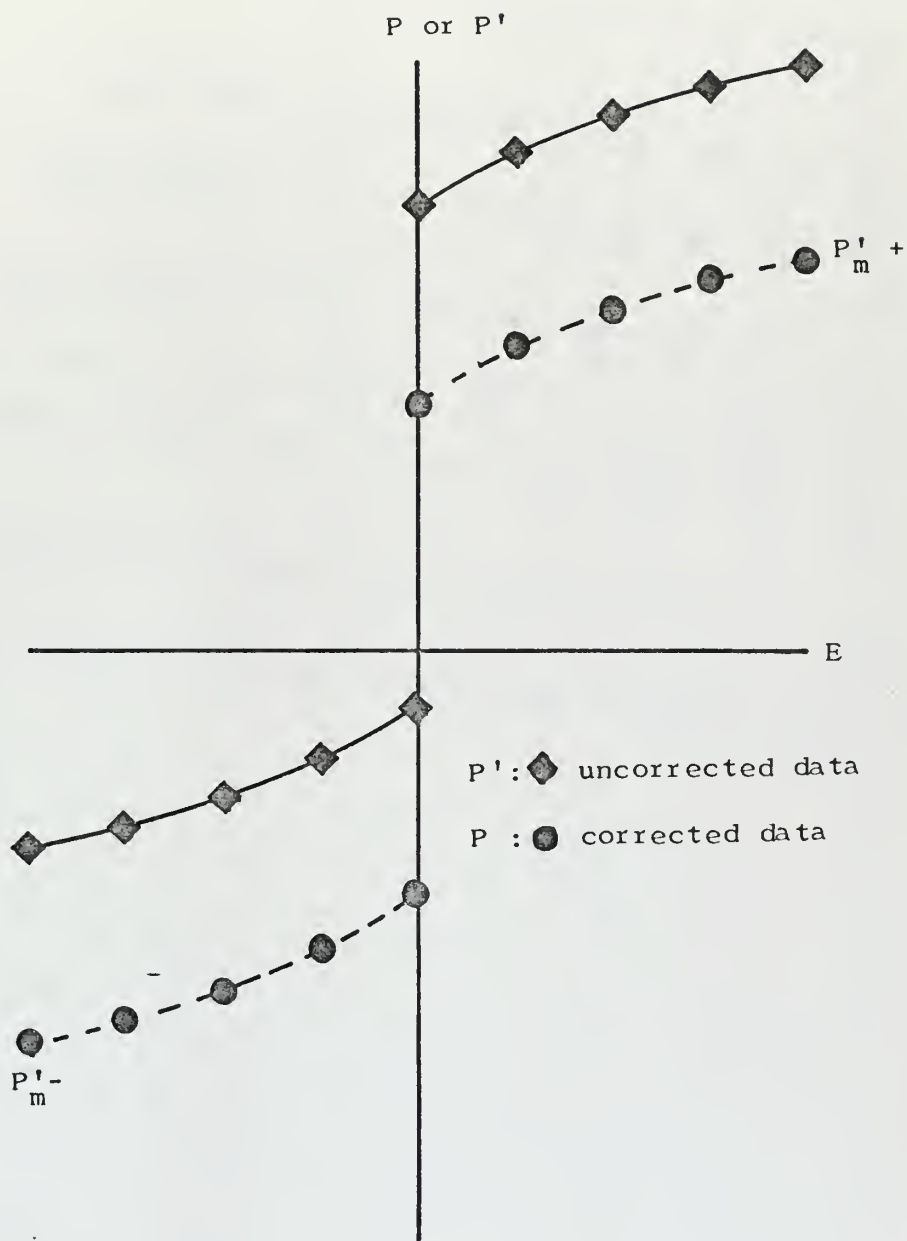
The initial polarity of the power supply for a data run was always chosen to be opposite to that last applied to the sample. The reason for this is that, even though the crystal was shorted at the end of a data run, it still retained a remanent polarization. If the next run was made with the same initial polarity as last applied to the sample, the value of the remanence becomes the zero for the next loop resulting in a strong bias. If instead, the opposite polarity is applied for the next run, the capacitor can be momentarily shorted after applying the initial voltage, allowing some charge to leak off and the loop can be approximately centered.

The thermistor resistance at T_c was located by very slow continuous heating of the sample through the transition. When the thermistor resistance became constant and then started to increase, indicating that the transition had been reached, the sample heater was turned off and the equilibrium resistance noted. This allowed correction for thermal lag between the bulk of the sample and the thermistor.

E.. DATA REDUCTION AND ERROR ANALYSIS

Before the raw electrocaloric data can be used, it must be adjusted to compensate for any bias of the hysteresis loop. This is done by assuming that the magnitude of the polarization for equal magnitude fields at the opposite ends of the loop is the same.. Subtracting the measured polarization at one end of the loop from the average of the magnitude at these two points gives a constant correction factor, which when added to the measured polarization at all other points on the loop, removes the bias. (See Figure 16.) Although the precision of the polarization measurements is 8×10^{-10} C/cm², the error in any measurement is $\pm 1\%$, due primarily to the inaccuracies in measurement of the sample dimensions.

Temperature changes were computed from the thermistor resistances by means of the relation $\Delta T = (1/R)(\Delta R/K)$. The precision of the resistance measurements was 10^{-3} ohm, leading to a temperature precision of 1.5×10^{-5} K. The error in an electrocaloric temperature change was $\pm 2 \times 10^{-4}$ K, due to thermal drift of the sample during the process of data accural. The error in $(T_C - T)$ is $\pm 1.2 \times 10^{-3}$ K, due to the difficulty in accurately determining the transition resistance. Complicated behavior associated with super-heating and supercooling occur at the transition, as described by Reese [31], making the choice of the transition resistance somewhat arbitrary, and an error of ± 0.1 ohm was assigned, leading to the error in $(T_C - T)$. For values of $(T_C - T) < 1.2 \times 10^{-3}$ K the error is less because it could be



$$\bar{P}_m = \frac{|P'_{m+}| + |P'_{m-}|}{2}$$

$$P = P' + (\bar{P}_m - P'_{m+})$$

Figure 16. Procedure for Normalizing Electrocaloric Polarization

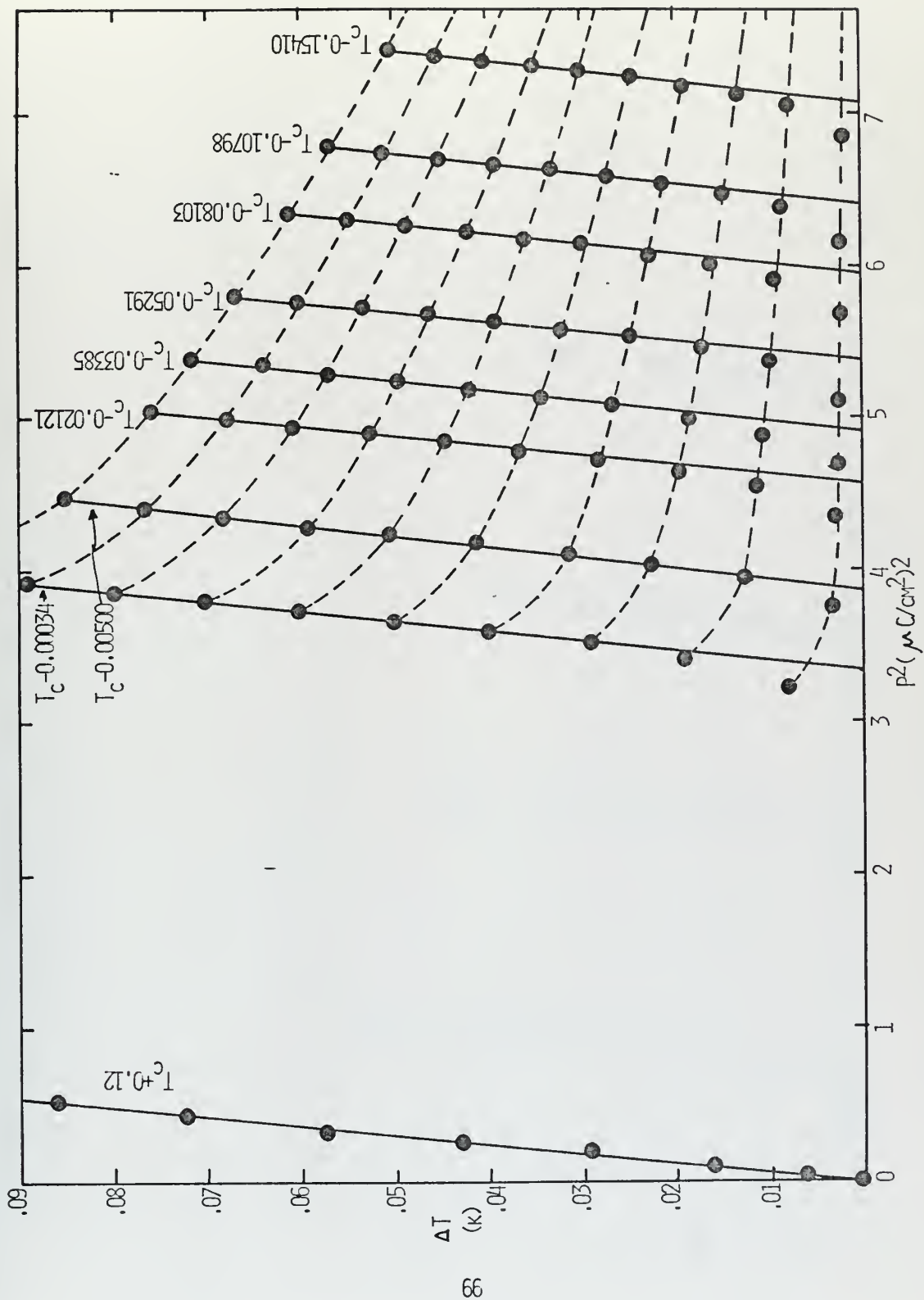


FIGURE 17A. p^2 vs ΔT DATA

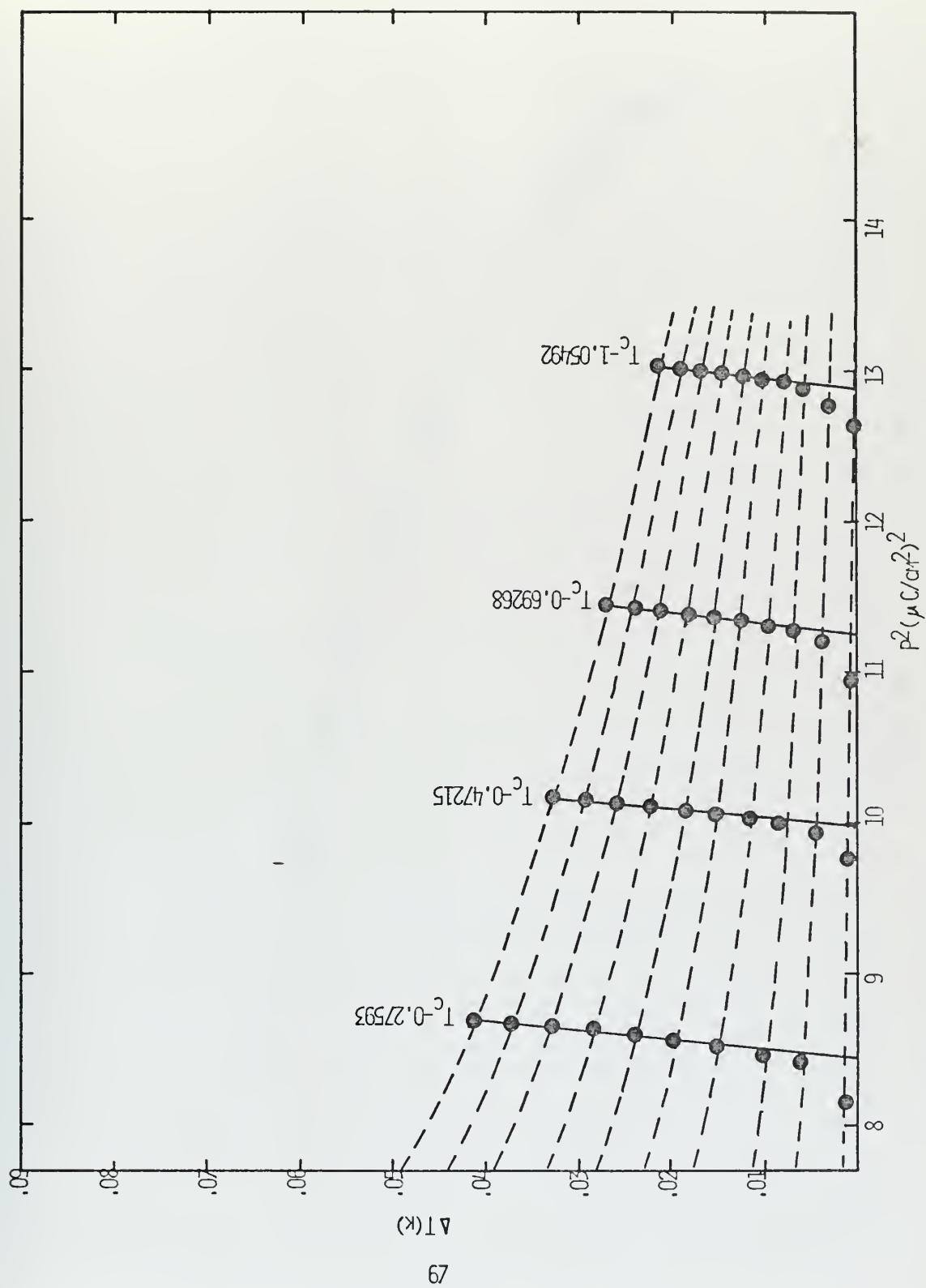


FIGURE 17B. p^2 vs ΔT DATA

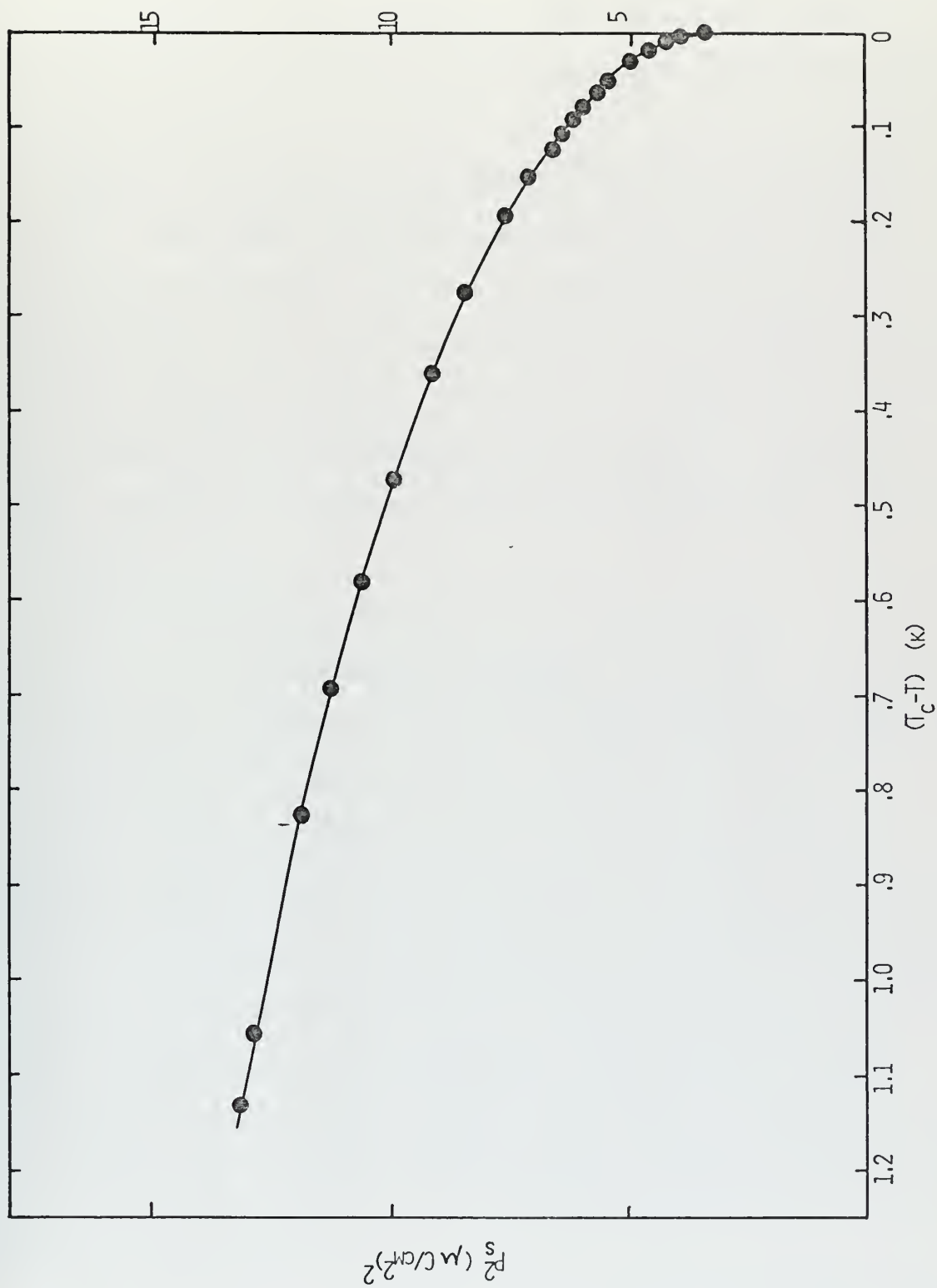


FIGURE 18. P_s^2 vs $(T_c - T)$

definitely ascertained that the sample was not through or in the transition region.

The precision of the electrical field measurements was 10^{-3} V/cm, again the imprecision in the sample dimensions caused an error of $\pm 1\%$.

Figure 17 shows the electrocaloric data cast in the form ΔT vs P_s^2 . The upper, saturated portion of the data is linear with very little scatter and can be extrapolated to get P_s^2 quite unambiguously. The expected deviation of the data from linearity at small values of ΔT due to the reversal of domains is present. The isochamps are also indicated in the figure by dotted lines. Figure 18 shows the resulting values for P_s^2 plotted as a function of $(T_c - T)$.

A second possible form in which to cast the data was a plot of ΔT vs E , for determination of $(\partial T / \partial E)_S$. This was tried, and it was found that the slope of the ΔT vs E data decreased slowly with the magnitude of the field, making it difficult to decide on a value for $(\partial T / \partial E)_S$. Since the data is to be used to calculate $\frac{\partial P_s}{\partial T}$ for comparison with the ΔT vs P_s^2 data, the value of $(\partial T / \partial E)_S$ at $E = 0$ was desired. To this end the differential slope of the data was plotted as a function of E . Some of the results are shown in Figure 19. Due to the scatter in the data a linear extrapolation to $E = 0$ was made and these values of $(\partial T / \partial E)_S$ used to calculate P_s . Figure 20 shows $(\partial T / \partial E)_S$ obtained in this fashion plotted against $(T_c - T)$.

The spontaneous polarization results obtained by these methods are presented and discussed in the next chapter.

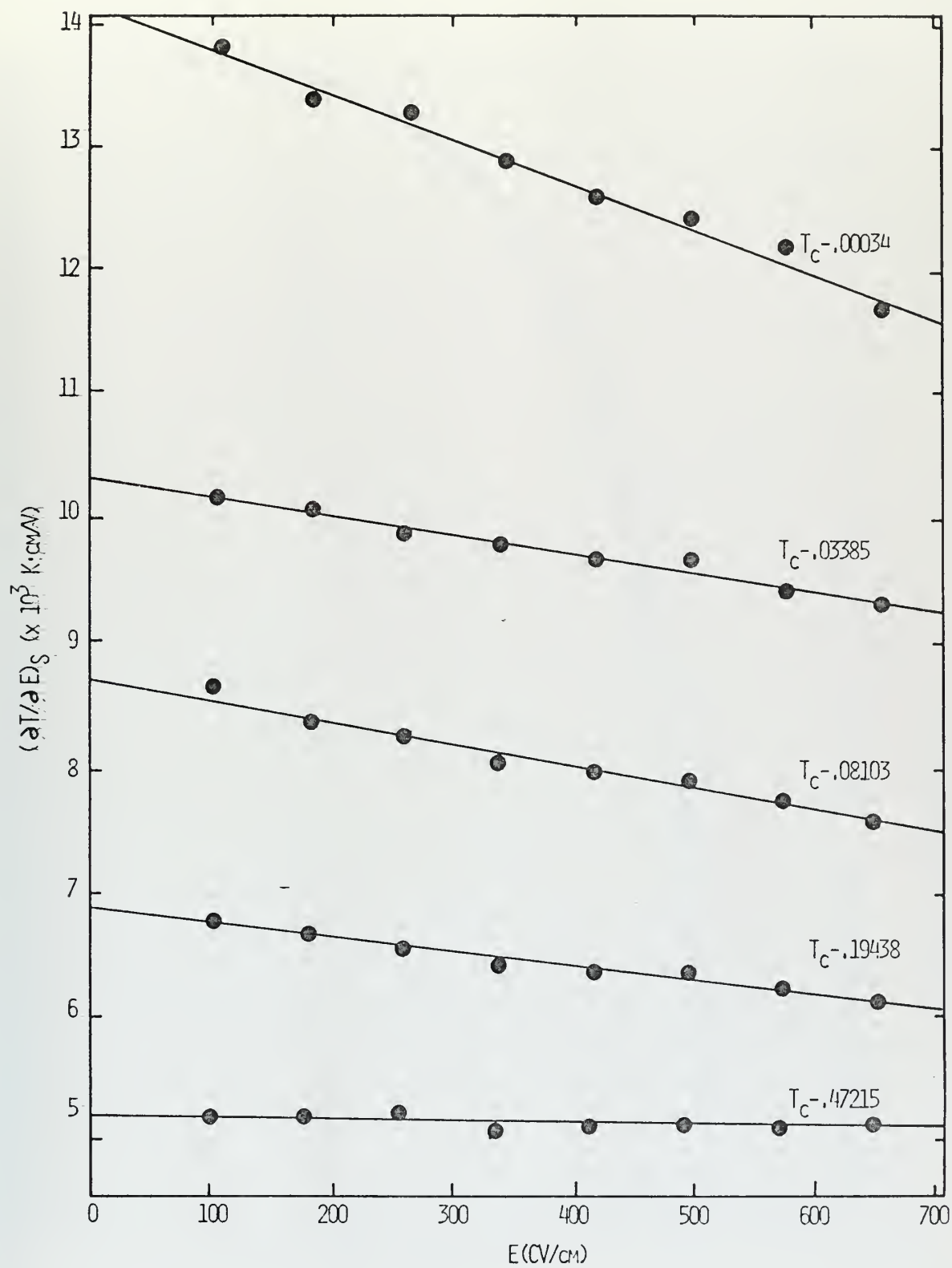


FIGURE 19. SOME $(dT/dE)_S$ VS E DATA

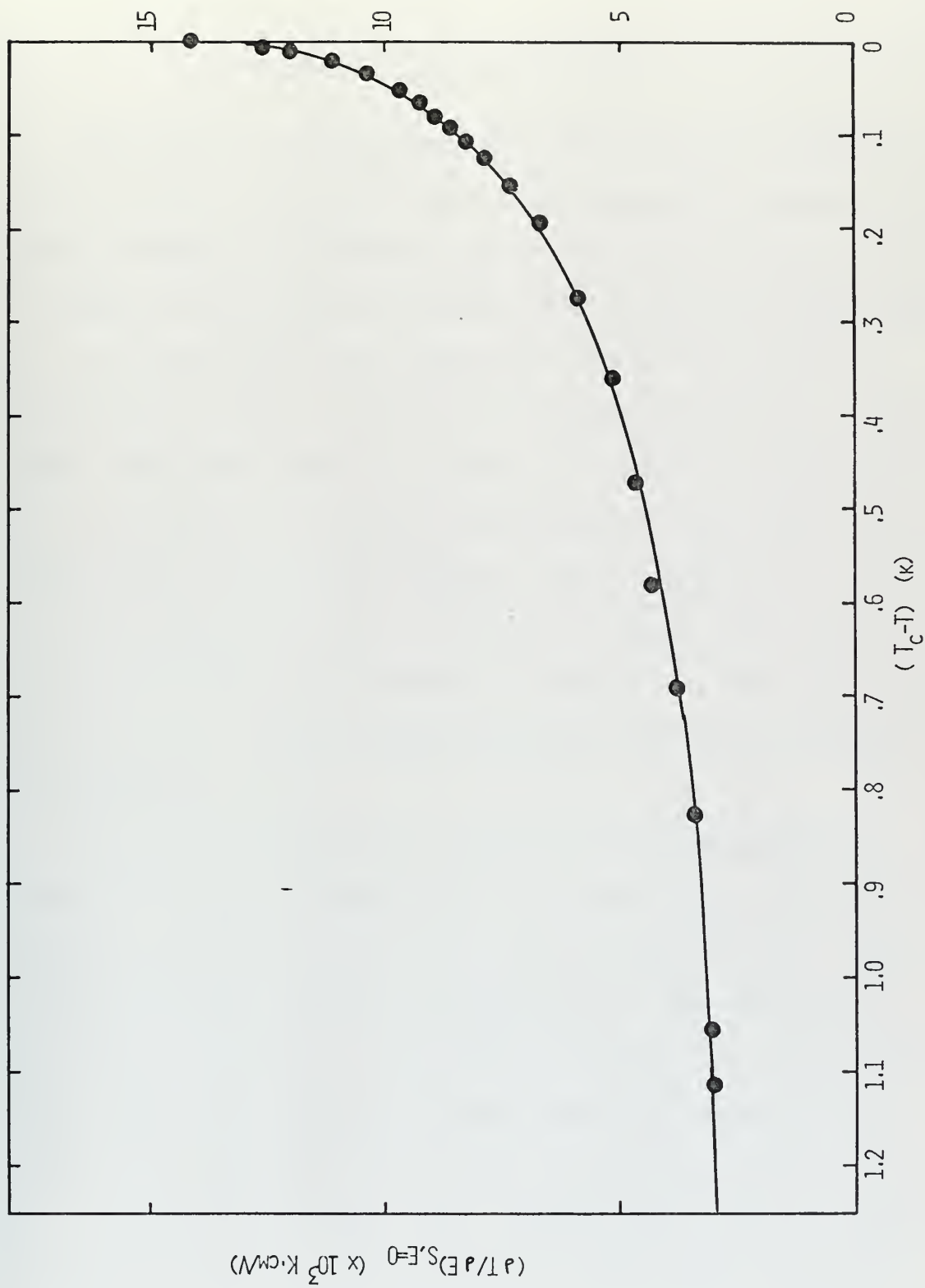


FIGURE 20. $(dT/dE)_S$ vs $(T_c - T)$

V. RESULTS AND CONCLUSIONS

Electrocaloric measurements were made only in the temperature region from T_c to $(T_c - T) = 1.1K$. The spontaneous polarization values obtained from extrapolation of the ΔT vs P^2 data are shown in Figure 21, where they are compared with the measurements made by von Arx and Bantle using dielectric hysteresis loops and De Quervain's values calculated from spontaneous strain measurements. The data connect to De Quervain's with fair agreement. The fit could be improved by normalizing his spontaneous strain measurements to our data to obtain a better value for b . There are quite large differences between the present data and that of von Arx and Bantle. As discussed in Chapter II, their data cannot be relied upon in this temperature region, so the disagreement is not significant.

The present measurements indicate that the ferroelectric transition in KDP is definitely first order, with a discontinuous jump in the polarization of $1.87 \pm 0.09 \mu C/cm^2$ at T_c . The uncertainty in this figure is primarily due to the difficulty in locating T_c accurately as was noted in Chapter IV. Using Landau theory (Eqn. (36), Chapter II) and Craigs [14] value for α , $3.457 \times 10^9 V \cdot cm/Clb \cdot K$, a value for the latent heat of $L = 42.9 \pm 4.3 J/mole$ was obtained. This compares very favorably with the value of 46.2 ± 4.5
 $- 6.0 J/mole$ obtained by Reese [32] from direct calorimetric measurements.

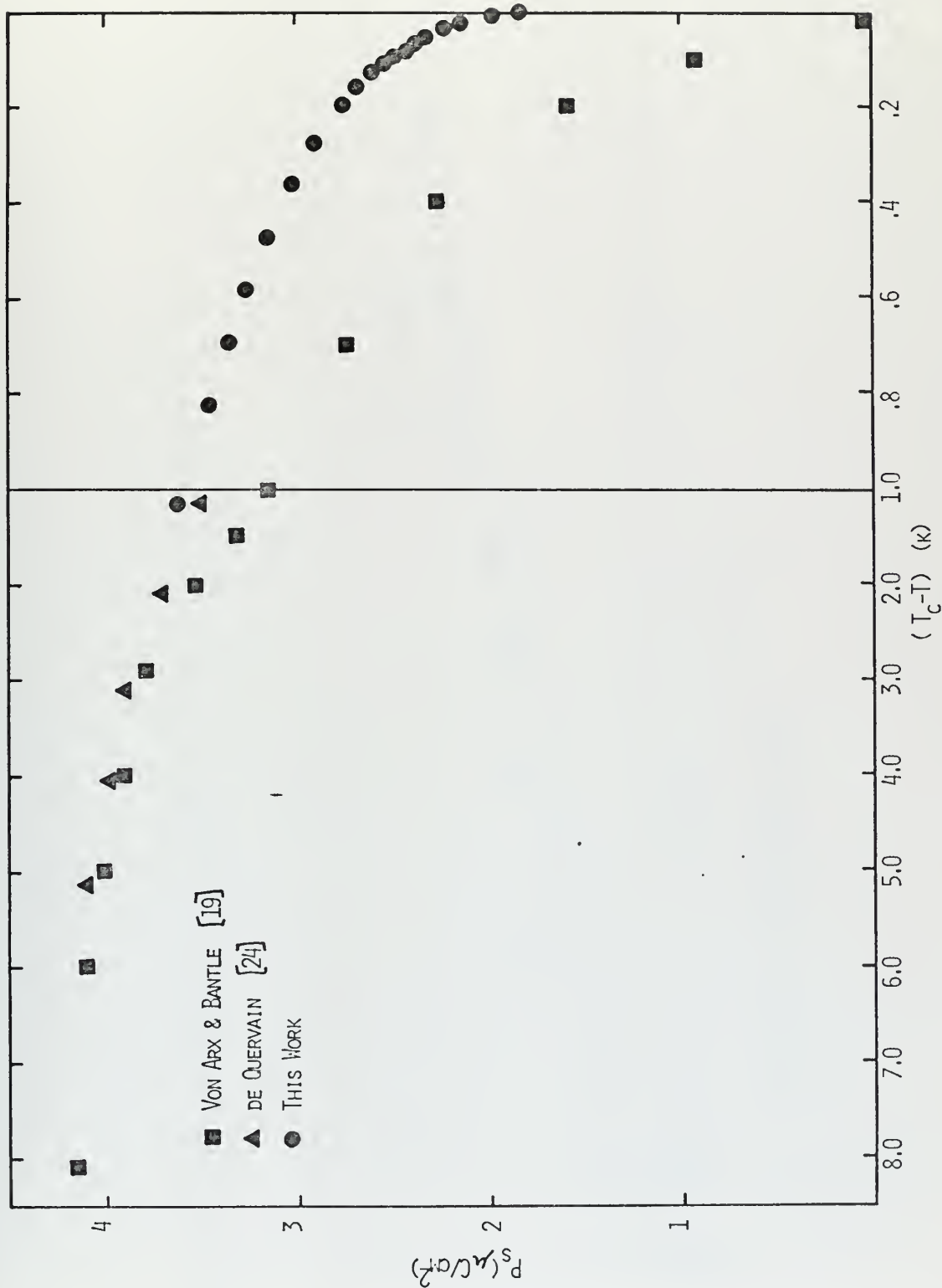


FIGURE 21. THE SPONTANEOUS POLARIZATION IN KH_2PO_4

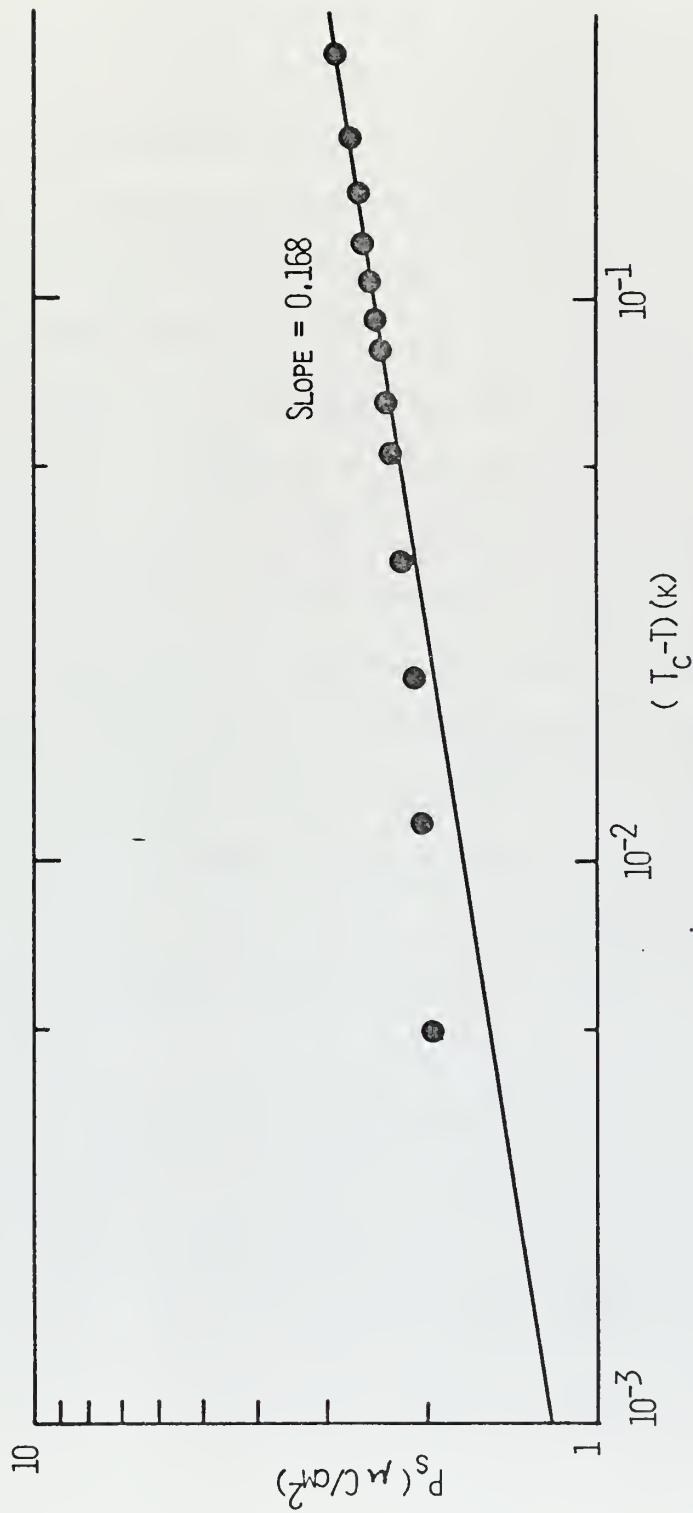


FIGURE 22. $\text{Log } P_s \text{ vs } \text{Log } (T_c - T)$

In Figure 22, $\log P_s$ is shown plotted against $\log (T_c - T)$. According to Eqn. (25), Chapter II, if the P^6 term in the free energy is the highest power term which cannot be neglected and if the magnitude of the coefficient β is "small" so that $\alpha\gamma/\beta^2$ is large, we should expect P_s to be proportional to $(T_c - T)^{1/4}$, and the slope of the data in the figure should be 0.25. Instead, we find a slope of 0.168 indicating that $P_s \sim (T_c - T)^{1/6}$. This implies that the P^8 term in the free energy is dominant. Taking this fact into account, the present data was fitted to Landau theory using a free energy function including the P^8 term and omitting the P^6 term for simplicity. The resulting equation for P_s (Eqn. (33), Chapter II) contains two free parameters, $P_s(T_c)$ and $(T_c - \theta)$. This equation was solved numerically, by iteration, for P_s using various values for the two parameters until a fit to the experimental data was found. In Figure 23, the experimental data and curve obtained from the best fit are shown. The agreement is excellent, indicating that the coefficient of the P^6 term in the free energy, γ , is very small and makes a negligible contribution to the free energy with 1K of T_c . The values of the two parameters which were used to obtain the best fit are $P_s(T_c) = 1.8716 \mu C/cm^2$ and $(T_c - \theta) = 0.012K$.

From these values for $P_s(T_c)$ and $(T_c - \theta)$, we can compute the coefficients β and δ . This was done using Craig's value for α in Eqns. (31a) and (31b) from Chapter II. The results are given in Table III in c.g.s. units for comparison with the values obtained by Reese [33] and Gladkii et.al. [34].

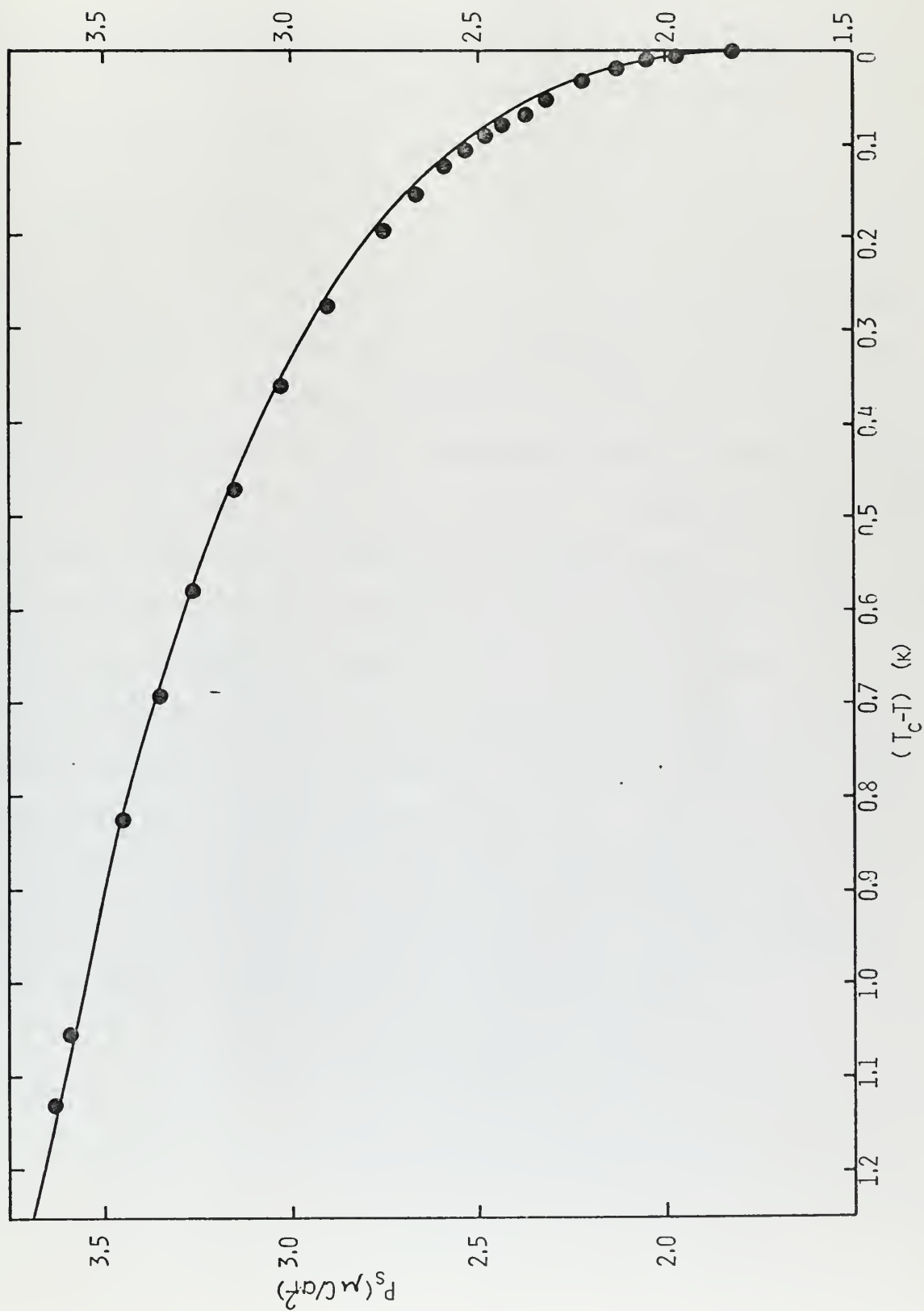


FIGURE 23. THE SPONTANEOUS POLARIZATION COMPARED WITH A TWO PARAMETER FIT TO LANDAU THEORY

TABLE III

Values for the parameters in the Landau expansion

Author:	This Work	Reese	Gladkii et.al.
α	3.846×10^{-3}	3.8×10^{-3}	2.4×10^{-3}
β	-4.399×10^{-12}	-1.88×10^{-12}	-4.0×10^{-11}
γ	0	3.97×10^{-19}	3.4×10^{-19}
δ	2.961×10^{-27}	1.04×10^{-27}	0

Note: Units are c.g.s.

Reese's values were obtained by fitting the "saturation function", $\Phi'(P)$, tabulated by Devonshire [17], keeping terms up to P^8 in the Landau expansion. Devonshire calculated his values from dielectric susceptibility and polarization measurements made by Baumgartner [35] in a small temperature region just above T_c . These polarization measurements were made by measuring the charge flowing from the sample as the polarity of the applied field was switched, using a ballistic galvanometer. This is a very insensitive method considering the response time of the galvanometer and the long time required for complete domain reversal. It should be expected that the polarization measurement will be too small. The susceptibility measurements were adiabatic because they were made at 1 KHz. Baumgartner used his polarization measurements to correct them to get the isothermal susceptibility via the equation:

$$1/\chi_S = 1/\chi_T + \alpha P^2 T / C_P .$$

Since Devonshire used the susceptibility measurements to calculate $\Phi''(P)$ and the polarization measurements to integrate it to find $\Phi'(P)$, the error in Baumgartner's polarization measurements is bound to be reflected in his values for $\Phi'(P)$. It is not surprising, then, that Reese's values for the expansion coefficients are not in agreement with those obtained from our data.

Gladkii et.al. measured $(\partial P/\partial T)_E$ as a function of various biasing fields above and below T_c . They obtain α from small signal, AC susceptibility measurements. Their value of 2.4×10^{-3} is almost a factor of two lower than any other previously determined value and cannot be accepted. The values obtained for the other two parameters are dependent on the choice made for α and so these results are not to be believed.

The values of the saturation function as a function of polarization for the present data and that of Gladkii et.al. were computed from:

$$\Phi'(P) = \beta P^3 + \gamma P^5 + \delta P^7.$$

They are shown in Figure 24 with the values tabulated by Devonshire. The lack of agreement of the various measurement is even more pronounced when cast in this form.

The thermodynamic consistency of our measurements was tested by computing the temperature derivative of our polarization measurements and comparing it with the value of $(\partial P/\partial T)_{E=0}$ obtained directly from the $(\partial T/\partial E)_S$ data via the equation:

$$(\partial P/\partial T)_E = - (T/C_E)(\partial T/\partial E)_S,$$

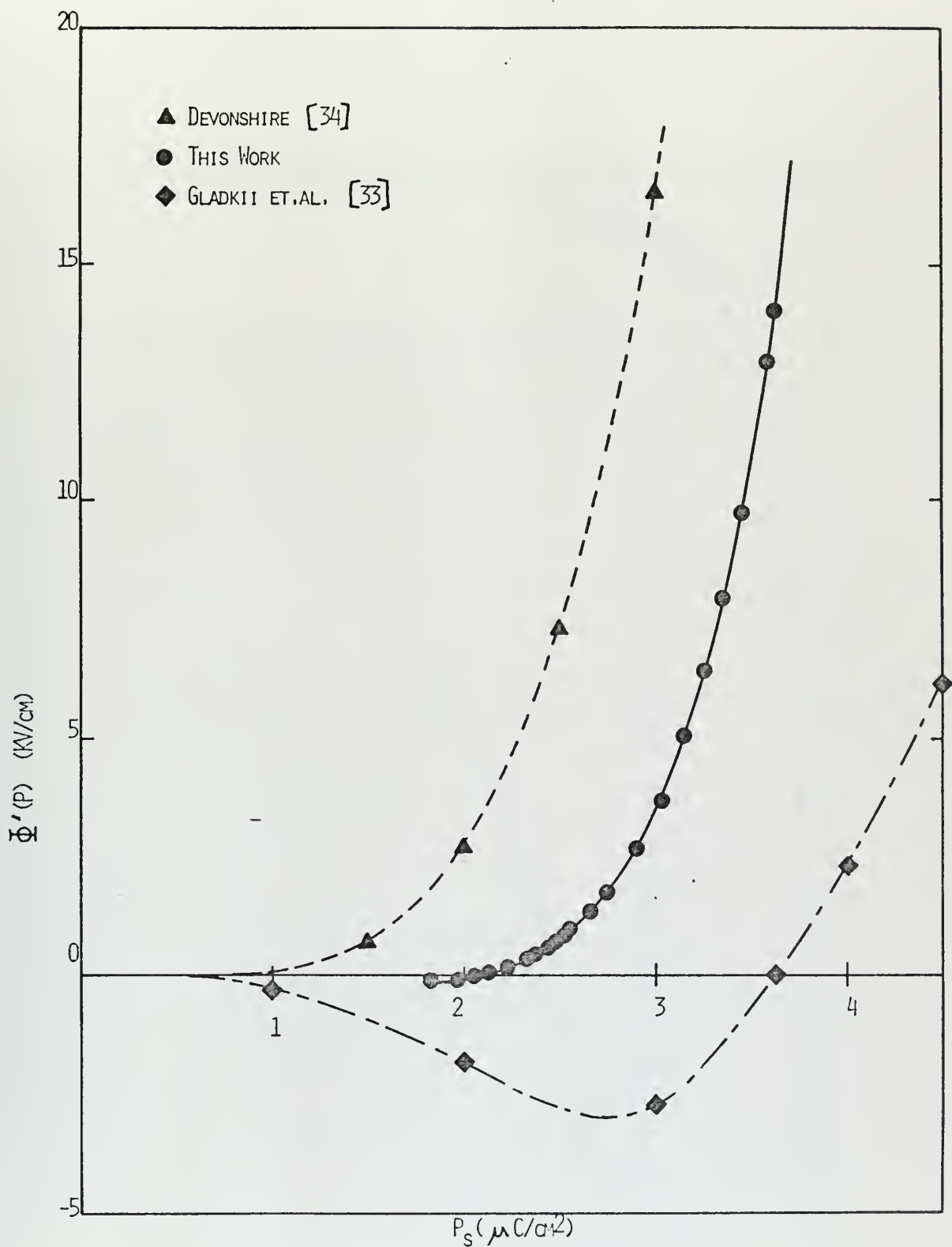


FIGURE 24. THE "SATURATION FUNCTION" IN KH_2PO_4

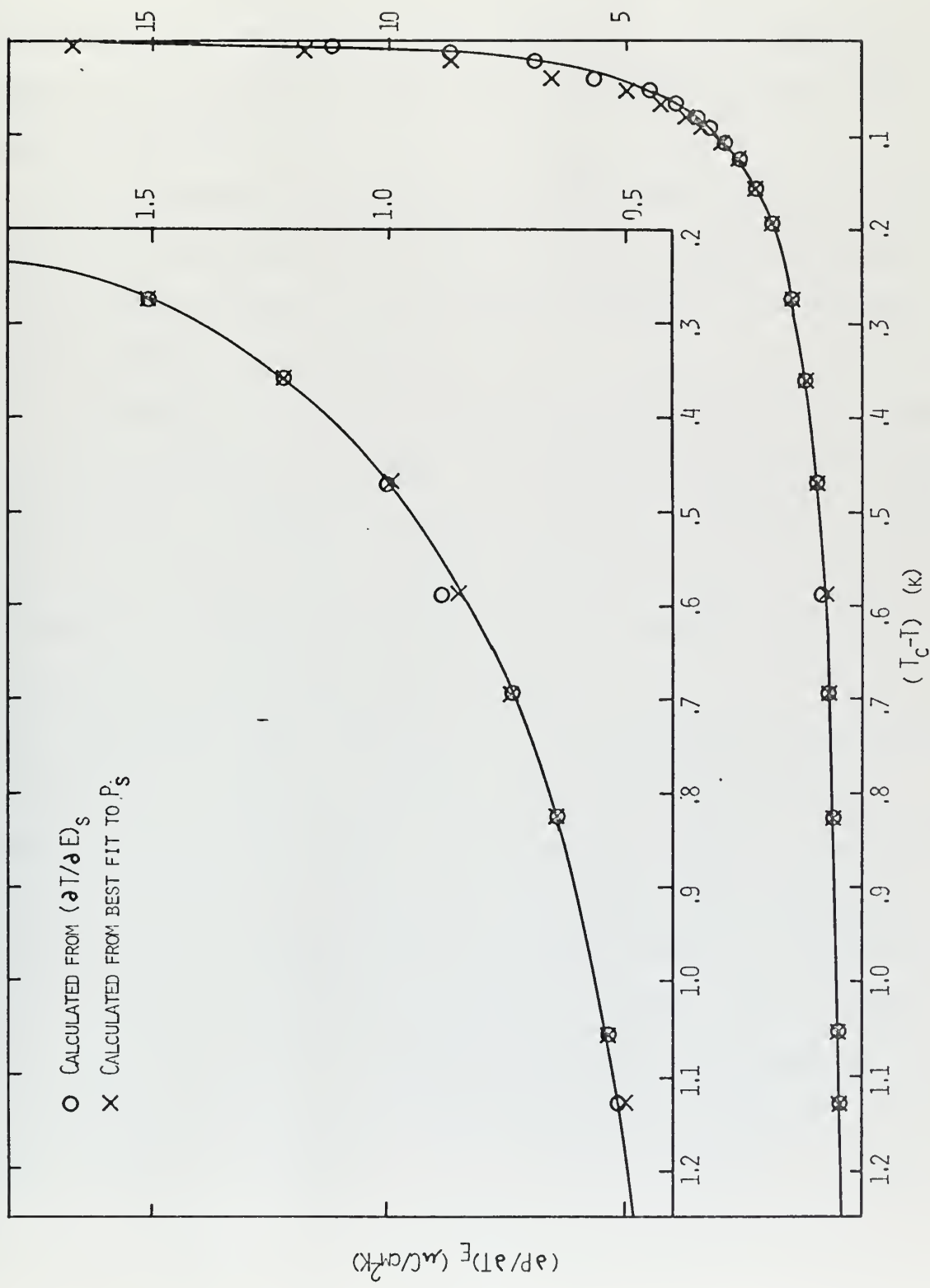


FIGURE 25. $(\partial P / \partial T)_E$ vs $(T_c - T)$

using Reese's values for C_E . The derivative of the polarization measurements was obtained by differentiating the two parameter fit to the data. The results of these calculations are shown in Figure 25. The agreement is excellent and indicates that our measurements are thermodynamically consistent. This comparison depends on thermodynamics alone and is independent of any theoretical assumptions.

As was explained in Chapter II, Landau theory allows the calculation of the specific heat from the data. Comparison of the calculations with other directly measured values allows a check on the validity of the theory.

The background specific heat C_P was calculated from the slopes of the ΔT vs P^2 data using Eqn. 42 and Craig's value for α . Below T_c there was a considerable amount of scatter in the data, so the average was taken. The value thus obtained was $C_P/R = 10.00 \pm 0.1$ where R is the universal gas constant. One data point was obtained above T_c , yielding $C_E/R = 8.98 \pm 0.1$ at $T = T_c + 0.12K$. At this temperature Reese obtains $C_E/R = 8.37$ by direct calorimetric measurements. Subtracting Reese's value from ours yields an addenda heat capacity (due to the thermistor, heater, electrodes, thread, and glue) of $0.61R \pm 0.2R$. This value falls within the range of values estimated for the addenda, based on previous calorimetric measurements employing similar addenda. Thus, this value was taken as the addenda contribution and used to correct the rest of the data, yielding $C_P/R = 8.37 \pm 0.3$ at $T_c + 0.12K$ and $C_P/R = 9.39 \pm 0.3$ below T_c .

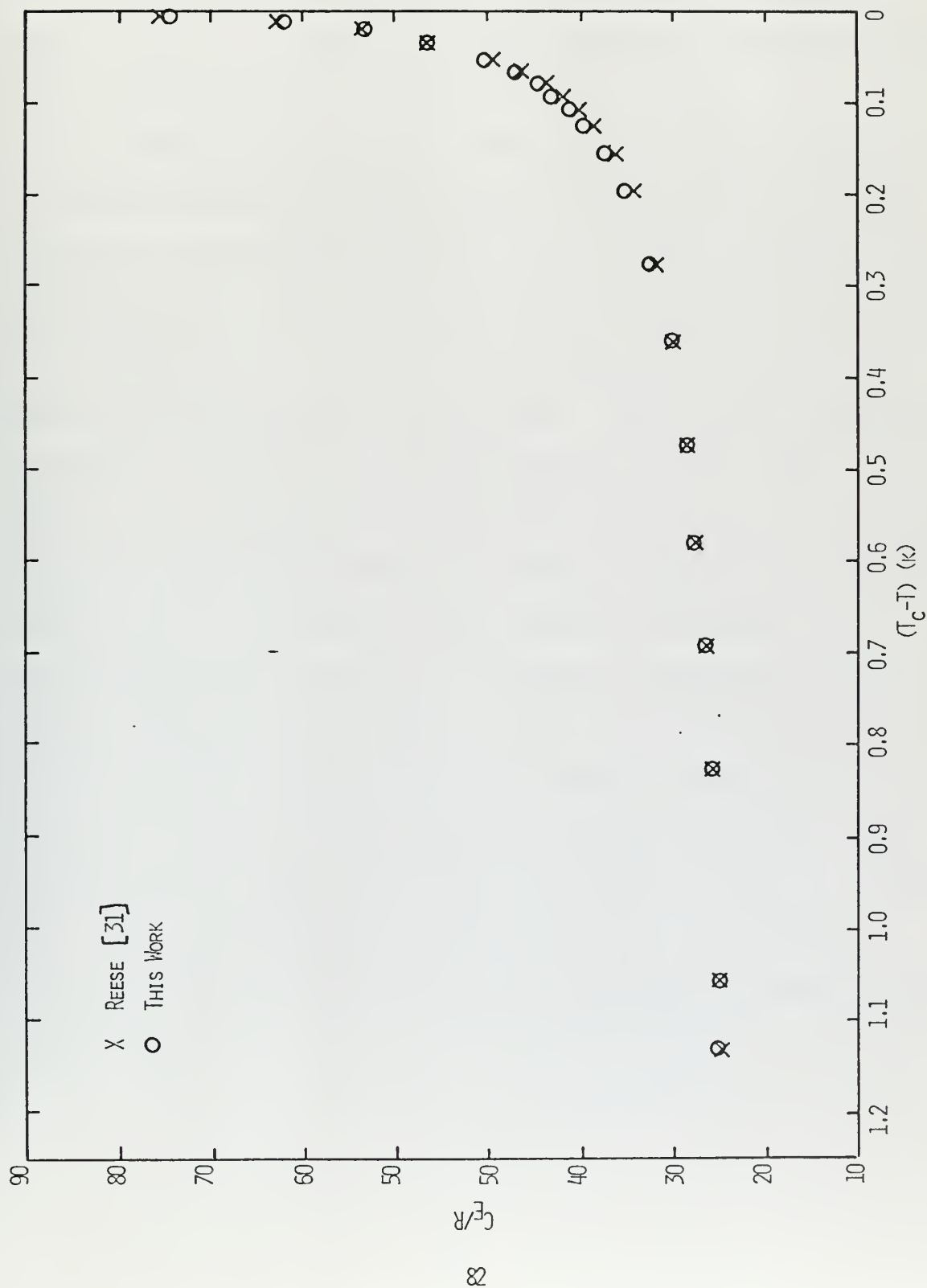


FIGURE 26. THE SPECIFIC HEAT IN $\text{K}_2\text{H}_2\text{P}_2\text{O}_7$

The total specific heat was calculated using Eqn. (40) with values for C_p and the polarization and $(\partial P/\partial T)_E$ obtained from the measurements reported here. The results of this calculation are shown in Figure 26 with Reese's measurements for comparison. The excellent agreement indicates that Landau theory is valid to within $10^{-3}K$ of T_c . This is further confirmed by the fit of Landau theory to the polarization data.

It should be noted that the value obtained for C_p/R below T_c is considerably larger than the value for C_E/R above T_c . From a comparison of the specific heats in KDP and deuterated KDP, Reese arrives at a value for the lattice background specific heat in KDP of $7.85R$ just below T_c . This is considerably smaller than the value of $9.39R$ calculated from our data. Since C_p , as measured by our method, represents all the specific heat of the sample not directly associated with the temperature dependence of the polarization, the difference between our value for C_p and that of Reese, combined with the agreement on C_E , indicates that some of the excess specific heat below T_c is associated either with proton ordering which is not correlated to the polarization or with a lattice anomaly. These considerations lead to the conclusion that Slater-type theories of the ferroelectric behavior of KDP cannot correctly predict both the specific heat and polarization, because they assume a one-to-one correspondence between the degree of ordering and the polarization and do not make any predictions about the lattice.

The measurements which have been reported here were made on three different samples with differing electrode characteristics, as described in Chapter IV. The only affect of the electrodes on the measurements if any should be to shift the Curie temperature as described in Appendix I. Since only temperature differences were measured no electrode effects should have been observed, and none were. The data from all three samples yielded consistent results.

In summary, we have reported what we feel are the most accurate spontaneous polarization measurements made in KDP to date. The measurements are shown to be thermodynamically consistent. Calculations of the specific heat using Landau theory agree extremely well with independent values obtained by direct calorimetric measurements. This indicates that Landau theory is valid to within 10^{-3} K of the transition. The transition is found to be first order. The differences between our measured lattice background specific heat and previous estimates indicate that the specific heat anomaly is not completely due to the temperature dependence of the polarization.

APPENDIX I

THE EFFECT OF STRESS DUE TO ELECTRODES ON THE FERROELECTRIC TRANSITION

A metal film which is evaporated onto the face of a KDP crystal well above the transition temperature will tend to resist the crystal deformation due to the piezoelectric strain which is induced by a field or exists spontaneously. We can approximate the effect of such a film by supposing that it acts like an external stress on the crystal, proportional to the strain. This is expressed by the equation:

$$X = - A x,$$

where A is a constant which depends on the properties of the particular film.

From Chapter II we have:

$$X = C^P x - aP,$$

and:

$$E = - bX + k^X_P + \Phi'(P).$$

Using the first two equations, we obtain:

$$X = - \left(\frac{a}{1 + \frac{C^P}{A}} \right) P.$$

Since a , C^P , and A are all constants, we define

$$B \equiv \frac{a}{1 + C^P/A},$$

and:

$$X = - BP.$$

Using this relation in the equation for the field we obtain:

$$E = (bB + k^X)P + \Phi'(P).$$

If we now assume that k^X does not change when $X \neq 0$, and use the stress free form:

$$k^X = \alpha(T - \theta).$$

We obtain:

$$\begin{aligned} E &= \alpha \left[T - \left(\theta - \frac{bB}{\alpha} \right) \right] P + \Phi'(P), \\ &= \alpha(T - \theta_X)P + \Phi'(P), \end{aligned}$$

where:

$$\theta_X = \theta - \frac{bB}{\alpha}.$$

We thus obtain the result that the effect of electrodes on the ferroelectric transition is to lower the transition temperature. As a check we see that as A becomes large, $B \cong a$, and:

$$\begin{aligned} E &= (ab + k^X)P + \Phi'(P), \\ &= k^X P + \Phi'(P), \end{aligned}$$

and we obtain the case of a clamped crystal, as we should.

Experimental evidence indicates that in a clamped crystal α is the same as for a free crystal and θ is shifted to a lower temperature. This justifies our assumption that k^X is unchanged by the presence of a stress.

APPENDIX II
EXPERIMENTAL DATA

$T_c - T$ (K)	P_s ($\mu\text{C}/\text{cm}^2$)	$(\partial T / \partial E)_S$ ($\times 10^{-5}$ $\text{K} \cdot \text{cm}/\text{V}$)	$(\partial P / \partial T)_E$ ($\mu\text{C}/\text{cm}^2\text{K}$)	$\Phi'(P)$ (KV/cm)	C_E/R
1.12931	3.628	2.970	0.513	14.013	14.87
1.05492	3.585	3.042	0.534	12.925	15.03
0.82616	3.450	3.467	0.645	9.710	15.94
0.69268	3.354	3.805	0.741	7.892	16.70
0.58090	3.261	4.364	0.892	6.413	17.96
0.47215	3.157	4.648	1.007	5.022	18.75
0.36034	3.025	5.191	1.218	3.643	20.24
0.27593	2.908	5.926	1.511	2.653	22.33
0.19438	2.757	6.729	1.925	1.738	25.02
0.15410	2.663	7.339	2.274	1.303	27.22
0.12531	2.593	7.838	2.615	1.016	29.36
0.10798	2.537	8.272	2.914	0.841	31.16
0.09202	2.483	8.615	3.222	0.697	32.95
0.08103	2.439	8.911	3.497	0.582	34.51
0.06562	2.375	9.240	3.935	0.440	36.91
0.05291	2.320	9.690	4.494	0.328	40.09
0.03385	2.223	10.406	5.645	0.168	46.34
0.02121	2.131	11.115	6.963	0.068	53.13
0.01175	2.051	11.918	8.728	-0.002	62.11
0.00500	1.976	12.610	11.169	-0.047	74.38
0.00034	1.827	14.158	19.370	-0.073	113.60

LIST OF REFERENCES

1. W. Cochran, *Advan. Phys.* 9, 387 (1960).
2. B.C. Frazer and R. Pepinsky, *Acta Cryst.* 6, 273 (1953).
3. G.E. Bacon and R.S. Pease, *Proc. Roy. Soc. (London)* A230, 359 (1955).
4. J.C. Slater, *J. Chem. Phys.* 9, 16 (1941).
5. Y. Takagi, *J. Phys. Soc. Japan* 3, 271 (1948).
6. Silsby et.al., *Phys. Rev.* 133, A165 (1964).
7. F. Jona and G. Shirane, Ferroelectric Crystals, Mac Millian (1962).
8. W. Känzig, Ferroelectrics and Antiferroelectrics, Solid State Physics, vol. 4, p. 1-197, Academic Press (1957).
9. E. Fatuzzo and W.J. Merz, Ferroelectricity, Wiley (1967).
10. J.C. Burfoot, Ferroelectrics, van Nostrand (1967).
11. B.A. Strukov et.al., *Phys. Stat. Sol.* 27, 741 (1968).
12. W. Reese and L.F. May, *Phys. Rev.* 162, 510 (1967).
13. S. Tsunekawa et.al., *J. Phys. Soc. Japan* 27, 919 (1969).
14. P.P. Craig, *Phys. Letters* 20, 140 (1966).
15. H. Mueller, *Ann. N.Y. Acad. Sci* 40, 321 (1940).
16. W.G. Cady, Piezoelectricity, McGraw-Hill (1946).
17. A.F.Devonshire, *Advan. Phys.* 3, 85 (1954).
18. L. Landau and E.M. Lifshitz, Statistical Physics, Permagon Press (1958).
19. C.B. Sawyer and C.H. Tower, *Phys. Rev.* 35, 269 (1930).
20. A. von Arx and W. Bantle, *Helv. Phys. Acta.* 16, 211 (1943).
21. I. Nazario and J.A. Gonzalo, *Solid State Comm.* 7, 1305 (1969).

22. R.E. Oettel, Unpublished Masters Thesis, Univ. of Washington, Seattle, (1964).
23. A. von Arx and W. Bantle, *Helv. Phys. Acta.* 17, 298 (1944).
24. G. Busch, *Helv. Phys. Acta.* 11, 269 (1938).
25. M. De Quervain, *Helv. Phys. Acta.* 17, 509 (1944).
26. F. Pockels, Lehrbuch der Kristalloptik, B.G. Teubner (1906).
27. B. Zwicker and P. Scherrer, *Helv. Phys. Acta.* 17, 346 (1944).
28. A.G. Chynoweth, *J. Appl. Phys.* 27, 78 (1956).
29. J. Azoulay et.al., *J. Phys. Chem. Solids* 29, 843 (1968).
30. G.G. Wiseman and J.K. Kuebler, *Phys. Rev.* 131, 2023 (1963).
31. B.A. Strukov, *Phys. Stat. Sol.* 14, K135 (1966).
32. W. Reese, *Phys. Rev.* 181, 905 (1969).
33. W. Reese, *Solid State Comm.* 7, 969 (1969).
34. V.V. Gladkii et.al., *J. Phys. Soc. Japan* 28, Supplement, 206 (1970).
35. H. Baumgartner, *Helv. Phys. Acta.* 23, 651 (1950).

INITIAL DISTRIBUTION LIST

	No. Copies
1. Defense Documentation Center Cameron Station Alexandria, Virginia 22314	2
2. Library, Code 0212 Naval Postgraduate School Monterey, California 93940	2
3. Assoc. Prof. G.E. Schacher Department of Physics Code 61 Naval Postgraduate School Monterey, California 93940	1
4. Assoc. Prof. W. Reese Department of Physics Code 61 Naval Postgraduate School Monterey, California 93940	1
5. Prof. O.B. Wilson, Jr., Chairman Department of Physics Code 61 Naval Postgraduate School Monterey, California 93940	1
6. LCDR John W. Benepe, USN COMCRUDESFLOT 8 FPO New York 09501	1

DOCUMENT CONTROL DATA - R & D

(Security classification of title, body of abstract and indexing annotation must be entered when the overall report is classified)

1. ORIGINATING ACTIVITY (Corporate author)

Naval Postgraduate School
Monterey, California 93940

2a. REPORT SECURITY CLASSIFICATION

Unclassified

2b. GROUP

3. REPORT TITLE

Measurements of the Spontaneous Polarization in KH_2PO_2

4. DESCRIPTIVE NOTES (Type of report and, inclusive dates)

Doctor of Philosophy Thesis; December 1970

5. AUTHOR(S) (First name, middle initial, last name)

John Wesley Benepe

6. REPORT DATE

December 1970

7a. TOTAL NO. OF PAGES

89

7b. NO. OF REFS

35

8a. CONTRACT OR GRANT NO.

b. PROJECT NO.

c.

d.

9a. ORIGINATOR'S REPORT NUMBER(S)

9b. OTHER REPORT NO(S) (Any other numbers that may be assigned this report)

10. DISTRIBUTION STATEMENT

This document has been approved for public release and sale; its distribution is unlimited

11. SUPPLEMENTARY NOTES

12. SPONSORING MILITARY ACTIVITY

Naval Postgraduate School
Monterey, California 93940

13. ABSTRACT

Measurements of the spontaneous polarization in KH_2PO_4 within 1K of the ferroelectric transition are reported. The measurements employed the electrocaloric effect, allowing simultaneous determination of the polarization and its temperature derivative. The derivative computed from polarization measurements compares well with direct determinations of $(\partial P / \partial T)_E$, demonstrating thermodynamic consistency of the measurements. The transition is first order with a discontinuous jump in the polarization of $1.87 \mu\text{C}/\text{cm}^2$ at the transition. Landau theory allows separate calculation of specific heat contributions of the lattice and polarization and thus the total specific heat, which agrees very well with direct calorimetric determinations, although the decomposition differs from that previously assumed. This indicates that Landau theory provides a good description of the transition in KH_2PO_4 and that there is a calorimetric anomaly not directly associated with the polarization. The free energy expansion best fitting the data contains P^4 and P^8 terms and no P^6 term.

KEY WORDS

LINK A

LINK B

LINK C

ROLE

WT

ROLE

WT

ROLE

WT

Ferroelectricity

Potassium Dihydrogen Phosphate (KH_2PO_4)

Spontaneous Polarization

Electrocaloric Effect

Specific Heat

Critical Point Phenomena

Phase Transition

Thesis

B367

c.1

Benepe

Measurements of the
spontaneous polariza-
tion in KH_2PO_2 .

123342

Thesis

B367

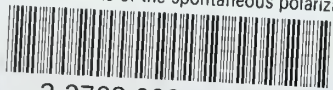
c.1

Benepe

Measurements of the
spontaneous polariza-
tion in KH_2PO_2 .

123342

thesB367
Measurements of the spontaneous polariza



3 2768 002 13021 3
DUDLEY KNOX LIBRARY